Università degli Studi dell'Insubria
Dipartimento di Medicina e Chirurgia
Dottorato in Medicina Sperimentale e Traslazionale
XXIX ciclo
Coordinatore: Chiar.ma Prof.ssa Daniela Negrini

ENDOMETRIAL CARCINOMAS WITH MISMATCH REPAIR DEFICIENCY: IMMUNOPHENOTYPICAL AND MOLECULAR CHARACTERIZATION

Relatore: Chiar.ma Prof.ssa Cristina Riva

Tesi di dottorato di:
Laura Libera
Matricola: 723108

Anno Accademico: 2015-2016

INDEX

INTRODUCTION

1. ENDOMETRIAL CARCINOMAS

The endometrial carcinoma (EC) is a neoplasia of the uterine corpus and isthmus that arises from glandular cells of Mullerian derivation. It represents the fourth most common cancer cause of death for women in the Industrialized Countries, suggesting that environmental and diet factors can increase the risk of endometrial carcinoma onset. The risk factors for endometrial cancer can include environmental, hormonal and hereditary-familiar factors (Lynch syndrome, LS) [1].

In 1983, Borkhman and colleagues hypothesized the existence of two different endometrial cancers types characterized by different pathogenesis [2, 3]:

- **Endometrioid carcinoma type I**, estrogen-dependent;
- **Non-endometrioid carcinoma type II**, not estrogen-dependent, represented by serous, clear cells, mucinous, squamous and undifferentiated adenocarcinoma.

The first group is characterized by a well differentiated histotype, low stage and it is associated to a good prognosis. The second group includes poorly differentiated carcinomas with rapid evolution and poor prognosis.

The molecular pathogenesis is different for the two groups: type I adenocarcinomas are mainly characterized by *PTEN* gene silencing, DNA repair system deficit (i.e. mismatch repair system, MMR) and mutations in *KRAS, CTNNB1* and *PIK3CA* genes [4]. On the contrary, type II serous adenocarcinomas show *TP53* mutations, p16 inactivation, low expression of E-cadherin and hyperexpression of HER-2. The immunophenotypical and molecular profile of clear cell carcinoma is not well defined yet, but recent data seem to focus the attention on *ARID1A* gene mutations [5].

In 2013, the Cancer Genome Atlas Research Network (TCGA) published a genomic characterization of 373 endometrial carcinomas (307 endometriod, 53 serous and 13 mixed endometrioid-serous) and defined a new classification of endometrial cancer based on biomolecular characteristics [6]. Four categories of endometrial cancer are described (Figure 1):

- ***POLE* ultramutated group**, characterized by *POLE* (DNA polymerase ε) mutations, high mutational load, rare copy number alterations, frequent C→A substitutions, *PTEN, PIK3CA, KRAS* mutations and good outcome;
- **MSI hypermutated group**, characterized by microsatellite instability (MSI) caused by mismatch repair (MMR) deficit due to hypermethylation of *MLH1*

promoter, high mutational load, rare copy number alterations, frequent *RPL22* frameshift deletions and *KRAS* and *PTEN* mutations;

- **Copy number low group**, usually endometrioid G1-G2, characterized by microsatellite stable profile (MSS, without MMR defect), low mutational load, frequent *CTNNB1* mutations;
- **Copy number high group**, serous-like, characterized by frequent copy number alterations, low mutational load, frequent *TP53, FBXW7* and *PPP2R1A* mutations, rare *PTEN* and *KRAS* mutations and poor outcome.

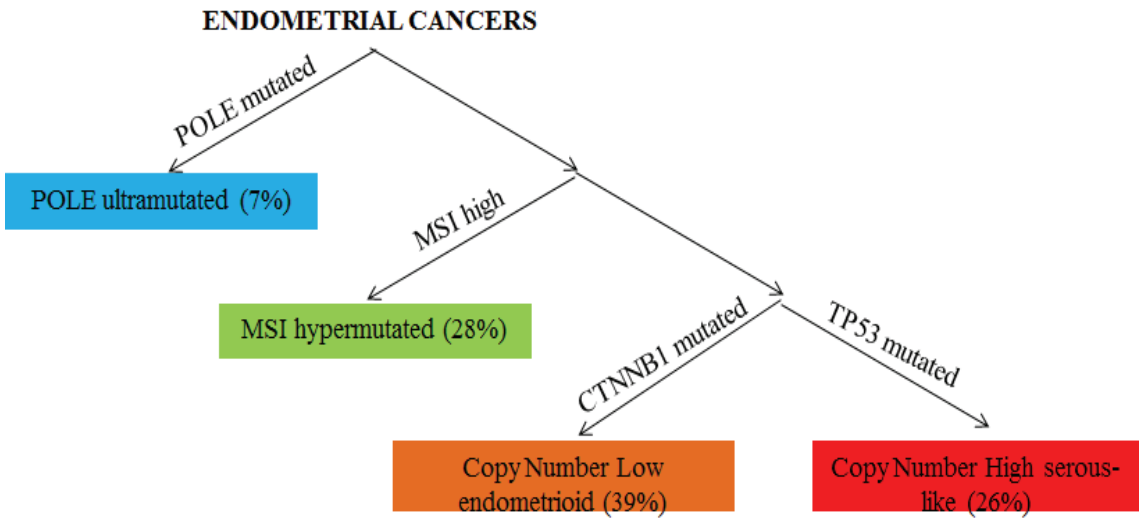

Figure 1. The Cancer Genome Atlas Research Network molecular classification.

In Table 1 the endometrial histotypes and their incidence are reported. The endometrioid carcinomas are the most frequent types and are estrogen-related; they are usually low grade (G1-G2, highly or moderately differentiated), which is scored based on the percentage of non-squamous solid areas (G1<5%, G2 6%-50% and G3>50%) [7]. The serous-papillary carcinoma is the not-endometrioid carcinoma prototype: it is rare (5-10% of all endometrial carcinomas), high grade (G3), frequently associated to myometrial and vascular invasion, about 75% of cases are stage III at clinical presentation (with peritoneal diffuse involvement and/or lymph node metastases) and they have worse prognosis. It can be caused by pelvic irradiation or prolonged therapy with tamoxifen and it can be associated to breast cancer. The clear-cell carcinoma is typically associated to high grade and advanced age and it has poor prognosis. It is more rare than serous carcinoma (2-4%) but it may have architectural features similar to serous carcinomas [8-10]. Finally,

mucinous, squamous, mixed and undifferentiated histotypes are less frequent (<1%) in endometrial site [11].

Table 1. Endometrial carcinomas histotypes and frequencies [12].

Histotype	**%**
Endometrioid adenocarcinoma	75-80%
Serous adenocarcinoma	<10%
Clear cell adenocarcinoma	2-4%
Mucinous adenocarcinomas	1%
Squamous carcinoma	<1%
Mixed carcinoma	<1%
Undifferentiated carcinoma	<1%

2. MISMATCH REPAIR SYSTEM

The human mismatch repair system (MMR) is a highly conservative enzymatic complex composed by several proteins. Its function is to recognize and repair erroneous misincorporation of bases that can arise during DNA replication and recombination, as well as to repair different types of DNA damage [13, 14]. The MMR system is composed by a heterodimer (MutSα or MutSβ) that recognizes the DNA mismatch and a heterodimer (MutLα, composed by MLH1 and PMS2 proteins) that removes and replaces the wrong nucleotide with the correct one, as shown in Figure 2. In detail, MutSα (composed by MSH2 and MSH6 proteins) recognizes single base mismatch and short DNA loops (shorter than 2bp), while MutSβ (composed by MSH2 and MSH3 proteins) recognizes bigger loops (from 3bp to 16bp) [15-18]. This process is ATP-dependent and requires the interaction of MMR system with exonuclease I and DNA polymerase δ [19-21].

MMR inactivation leads to the accumulation of errors in highly repetitive sequences, such as microsatellite repeats, resulting in a peculiar phenotype called microsatellite instability or MSI [22]. Recent works have identified more than 60 target genes, containing microsatellite sequences, which are involved in transduction pathways, cell cycle control, growth regulation, apoptosis and DNA repair [14].

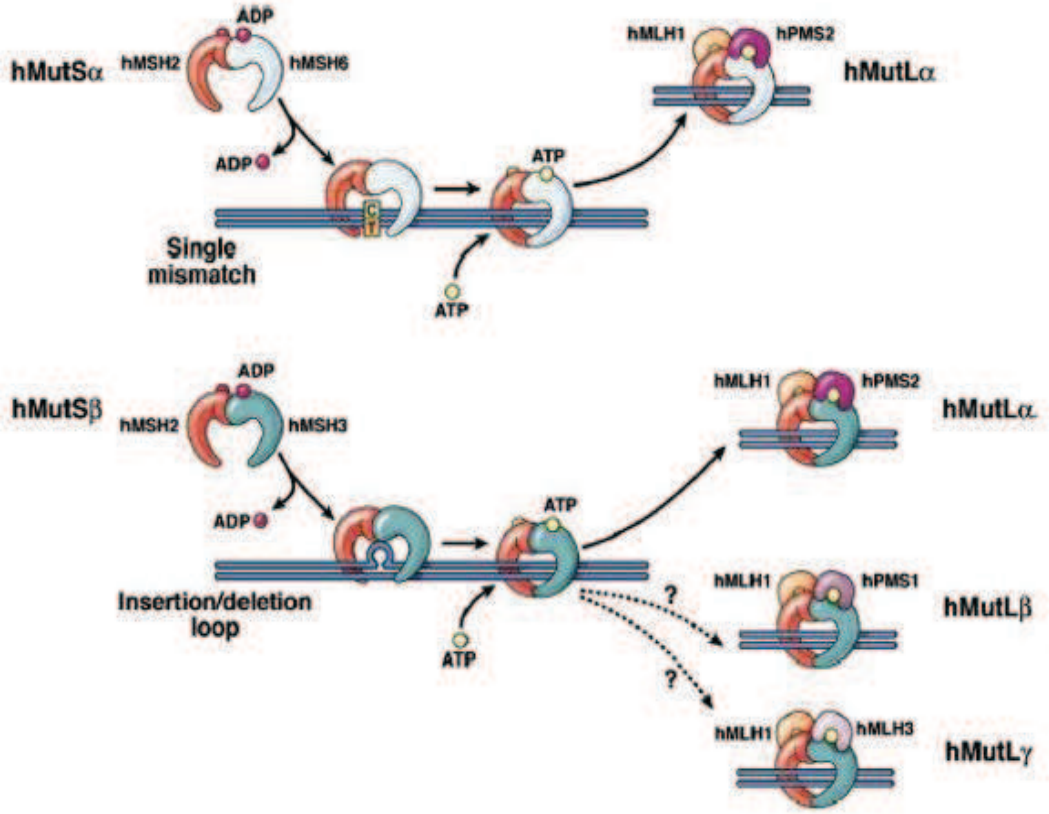

Figure 2. MMR proteins interaction during the repair of replication errors [14].

3. SPORADIC ENDOMETRIAL CANCER WITH MMR DEFICIENCY

MMR deficiency and MSI phenotype occur in almost 30% of sporadic endometrial tumors [23]. The majority of these tumors shows the inactivation of *MLH1* gene, which mostly results from promoter hypermethylation rather than somatic mutations or loss of heterozygosity [24-27].

In detail, the silencing event is caused by hypermethylation at CpG sites of *MLH1* promoter as described by Deng et al [28, 29]. Deng and colleagues divided the *MLH1* promoter in four regions [A region (from -711 to -577, containing 23 CpG sites), B (from −552 to −266, 19 CpG sites), C (from −248 to −178, 8 CpG sites), and D (from −109 to +15, 7 CpG sites)] and correlated the methylation status of each region to the MLH1 protein expression. Finally, they concluded that methylation status of CpG sites in region C provided the best correlation and prediction of *MLH1* expression, while methylation in

region A seemed not to be critical in silencing the gene expression. It was also suggested that methylation in regions B and D could be important in silencing *MLH1* expression, but methylation in these regions did not provide the best correlation between the methylation status and *MLH1* expression.

Recently, Bosse and colleagues identified a correlation between *MLH1* methylation and immunohistochemical loss of ARID1A protein [5, 30]. The switch/sucrose non-fermentable (SWI/SNF) subunit *ARID1A* (AT-rich interactive domain 1A) is a tumor suppressor gene located on chromosome 1p36.11 and encodes for a core member of SWI/SNF complex [31, 32]. This complex is involved in chromatin remodeling, which is a molecular mechanism of regulation of gene expression levels based on ATP-dependent changes of nucleosome structure and plays a crucial role in carcinogenesis [32]. *ARID1A* presents four important domains: a DNA-binding domain (ARID domain) that can specifically bind an AT-rich DNA sequence; a SWI/SNF interaction domain that interacts with SMARCB1 or SMARCA4, two SWI/SNF subunits; a HIC1-binding domain that binds HIC1 (hypermethylated in cancer 1 protein); a C-terminus domain that can activate glucocorticoid receptor-dependent transcription (Figure 3) [33]. Inactivating *ARID1A* mutations (usually frameshift or nonsense) lead to cancer progression by alterations of cell differentiation, migration, adhesion and cell cycle timing [34, 35].

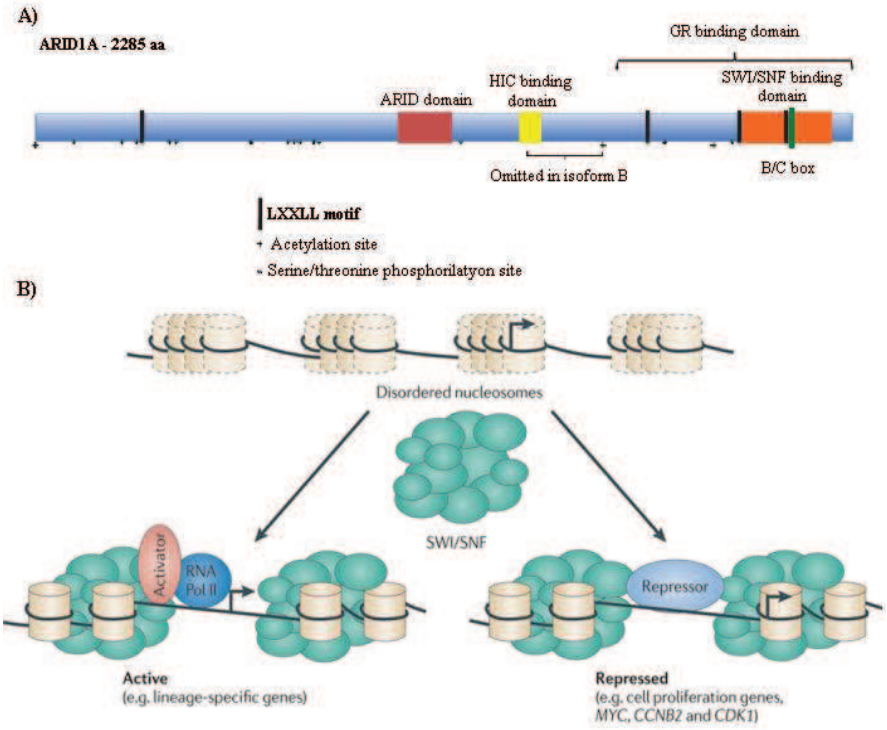

Figure 3. A) *ARID1A* structure domains; B) SWI/SNF complex in activation or repression of gene transcription.

LYNCH SYNDROME AND ENDOMETRIAL CANCER

Lynch syndrome (LS, ORPHA 144, OMIM #120435) is a hereditary disease with autosomal dominant transmission and high penetrance (80-85%) characterized by high genetic heterogeneity. It is caused by a germline inactivating mutation in one tumor suppressor gene that encodes for a protein of MMR system, namely *MLH1, MSH2, MSH6* and *PMS2* [36, 37].

To date, more than 2360 MMR germline variants have been identified and enclosed in the international database called *InSiGHT* (International Society for Gastrointestinal Hereditary Tumours) [38]. These genes do not display any mutational hot spot, as a matter of fact the mutations are distributed along the whole gene. *MLH1* and *MSH2* genes are more frequently mutated (40% *MLH1* e 34% *MSH2*), followed by *MSH6* (18%) and *PMS2* (8%) [39]. The *InSiGHT* has recently classified the germline variants in five classes based on the clinical significance [38] (www.insight-group.org): **class 1**, not pathogenic; **class 2**, likely not pathogenic; **class 3**, variants with uncertain significance (VUS); **class 4**, likely pathogenic; **class 5**, pathogenic.

Most of MMR germline mutations generate a stop codon and a non-functioning truncated protein [40]. On the contrary, one third of missense variants is VUS and additional tests, such as *in silico*, functional and segregation assays, are needed to better define the clinical significance of VUS (according to *InSiGHT* guideline, www.insight-group.org).

As reported in literature, the MMR inactivation model follows the Knudson's two hit hypothesis [41]. In LS tumors, the "first hit" is represented by a germline mutation (point mutation or large rearrangement), while the "second hit" is acquired at somatic level due to different genetic mechanisms (deletion, mitotic recombination, point mutation, genetic conversion, loss of heterozygosity) [42]. Recently, Lynch patients with a germline epimutation of *MLH1* or *MSH2* have been described in literature [43]. Epimutations are defined as changes that do not involve primary gene sequence, but include epigenetic modifications that finally alter the transcription of the gene [42, 44]. The principal epigenetic mechanism is cytosine methylation/demethylation in CpG sites of a gene promoter [44-47]. In literature, two types of constitutional epimutations are reported:

- **primary epimutation** is a modification arising *de novo* in a patient, reversible between generations and then not necessarily heritable;

- **secondary epimutation** is caused by a cis-acting genetic-based alteration, and shows a autosomal dominant inheritance pattern.

As reported by Peltomaki and colleagues, secondary epimutation of *MLH1* gene can be caused by a deletion in *MLH1* 5'-UTR, a SNP in *MLH1* promoter or a large duplication that includes *MLH1* gene and its flanking regions. The "second hit" after an epimutation is usually the somatic loss of heterozygosity of the wild-type allele [42]. Secondary epimutation of *MSH2* can be the result of a deletion of 3'-UTR region of the closely linked *EpCAM* gene [48]. *MSH6* and *PMS2* epimutations have never been reported.

In LS patients with colorectal cancer, the frequency of constitutional epimutation ranges from 2% to 13% for *MLH1* and 0%-9% for *MSH2* [49, 50].

LS patients are characterized by cancer onset in different sites at younger age compared with normal population. The tumor spectrum includes colorectal (CRC, 35-55%), endometrial (10-45%), ovarian, stomach, pelvic tract, hepatobiliary tract and small bowel cancers [51]. In 2005, Lu et al observed that 50% of LS women, affected by endometrial and colorectal cancers, showed the endometrial cancer as first manifestation of the syndrome, so it was defined as LS "sentinel cancer" [52]. In literature, different cancer risks are reported based on which *MMR* gene is mutated. For instance, a woman carrying a *MSH6* germline mutation would more likely develop endometrial cancer with respect to colorectal cancer, in comparison with patients carrying a *MLH1* or *MSH2* germline mutation [53-55]. Interestingly, *PMS2* mutation carriers have 15% of cancer risk to develop CRC, 15% for EC and 25-32% of risk to develop other LS tumors up to 70 years of age [56].

The histopathology of LS associated endometrial tumors is typically endometrioid, but also serous, clear cells and mixed histotypes are observed. Carcangiu et al. observed a higher number of non-endometrioid histotypes in LS women with respect to non-syndromic women (43.5% vs 4.3% respectively) [57]. On the other hand, Garg and Soslow suggested that undifferentiated and dedifferentiated endometrial carcinomas are frequently associated with mismatch repair abnormalities and Lynch syndrome in addition to the endometrioid classical histotype [58]. Moreover, these ECs are characterized by an abundant "Crohn-like" lymphocyte infiltrate [53].

DETECTION OF MMR DEFICIENT ECs IN ROUTINE DIAGNOSTICS

The recognition of ECs with MMR deficiency is very important in routine diagnostics for several reasons.

First, in the sporadic endometrial carcinogenesis the prevalence of MMR deficient ECs represents approximately 20-30% of all endometrial carcinomas [23, 59, 60]. In particular, patients that display a MMR deficient ECs show a better prognosis in comparison to patients with MMR proficient ECs [59, 60]. Indeed, Kato and colleagues observed a five-year progression free survival of 92% in MMR deficient tumors with respect to 78% in MMR-retained cases and a five-year overall survival of 94% for MMR-deficient tumors in comparison to 78% for MMR proficient tumors. Moreover, patients with MMR deficient tumors may benefit from immunotherapy [61]. Recently, it was demonstrated that neoplasms with a strong host immune response against cancer cell, such as melanoma and lung cancer, are greatly sensitive to PD-1 (Programmed cell death protein 1) inhibitors. MSI tumors are hypermutated and express many frameshift peptides which act as neoantigens that elicit an immune response by tumor-infiltrating lymphocytes [62]. Thus, when PD-1 is inhibited, the lymphocytes at the tumor border are activated and attack the tumor.

Secondly, a subset of MMR deficient ECs are associated to Lynch syndrome. The identification of LS patients is crucial as they have a higher risk of recurrence and cancer onset in other sites compared to normal population and they should refer to a specific program of prevention and surveillance [36, 52].

In routine diagnostics, the MMR deficiency tests consist in the immunohistochemical (IHC) evaluation of the MMR proteins expression and/or the microsatellite instability (MSI) analysis. The critical aspects of IHC test regard mainly the careful evaluation of internal normal controls, the evaluation of cases with focal/patchy expression of the proteins and the recognition of staining artifacts caused by technical problems [63].

On the other hand, the MSI test is less sensitive than MMR IHC analysis [64], probably due to the evaluation of microsatellite loci which are not specific for endometrial site but only for the gastrointestinal tumors [65] or to biological characteristics of the endometrial cancers which are less unstable, as recently described in a complete NGS microsatellite analysis of cancers belonging to 18 different anatomical sites [66].

To date, two main panels are being used for the MSI analysis: the Bethesda panel and a mononucleotide repeats pentaplex (MRP) panel suggested by Suraweera et al. [67, 68].

The Bethesda panel includes two mononucleotide repeats (BAT-25 and BAT-26) and three dinucleotide repeats (D5S346, D2S123 and D17S250) which are highly polymorphic in the population, thus they require the analysis of the corresponding germline DNA [67]. Moreover, the interpretation of size alterations in dinucleotide repeats is difficult and can lead to misclassification [69].

The MRP panel, instead, consists in five mononucleotide repeats (BAT-25, BAT-26, NR-21, NR-22 and NR-24) which have a very low frequency of polymorphisms in Caucasian population and do not require the corresponding germline DNA for comparison [68]. Additionally, recent works suggest the evaluation of new microsatellite instability loci which have been identified in endometrial tumors, in order to improve the sensibility of microsatellite instability analysis in ECs [70-73].

AIM

The operative work of my PhD training in Experimental and Translational Medicine has been carried out at the Unit of Anatomical Pathology of Varese Hospital. During my doctoral training, we selected a series of 80 gynecological cancers (mainly represented by endometrial cancers) belonging to 76 patients who referred to the Oncological Genetic Counseling Service of Varese Hospital with a suspect of Lynch syndrome.

The aim of my doctoral thesis included:

1. the identification of gynecological cancers (GCs) with mismatch repair (MMR) deficiency using different somatic tests, including the immunohistochemical evaluation of mismatch repair proteins and the microsatellite instability analysis;
2. the evaluation of EC-specific microsatellite loci in order to improve the sensitivity of MSI analysis;
3. the identification of hereditary and sporadic MMR deficient GCs using MMR germline mutation analysis and *MLH1* promoter methylation test;
4. the molecular characterization of 35 endometrial cancers using a targeted exome sequencing of 16 genes involved in endometrial carcinogenesis.

MATERIALS AND METHODS

1. Patients and samples

We studied 80 formalin fixed and paraffin embedded (FFPE) gynecological cancers (GCs) of 76 patients collected in the last 15 years at the Unit of Pathology of Varese Hospital. All patients referred to Cancer Genetic Counseling Service of Varese hospital with the suspect of Lynch syndrome (LS) due to a positive family history and/or the manifestation of synchronous/metachronous uterine and ovarian cancers, according to Bethesda revised and Amsterdam criteria. For this reason, the series included 63 endometrial carcinomas (59 cases localized in corpus/fundus region and four cases at the isthmus level), 13 ovarian cancers and four endocervical carcinomas for completeness (Table 2).

Two independent pathologists reviewed the histological diagnosis of all samples according to the 4th edition WHO classification of tumors of the gynecologic tract and the TNM staging system [74]. The grade of differentiation was evaluated in agreement with the 7th edition of AJCC manual [75].

As shown in Table 2, the series of 80 GCs was composed by 64 endometrioid, eight mixed (endometrioid and serous), two serous, two clear cell, two undifferentiated, one mucinous histotypes and one carcinosarcoma. Comprehensively, the series included 59 low grade tumors (27 G1 and 32 G2) and 19 high grade tumors.

Clinico-pathological informations of all 80 tumors are summarized in Table 2.

Table 2. List of 76 patients and the corresponding 80 gynecological cancers.

Patient ID	Tumor ID	Age of onset	Site	Histotype	pT	pN	Grade
1	1	53	Endometrium	Endometrioid	1a	0	2
2	2	42	Ovary	Serous	-	-	3
3	3	47	Endometrium	Endometrioid	1a	0	1
4	4	47	Endocervix	Endometrioid	1b	0	2
5	5	55	Endometrium	Endometrioid	1a	0	1
6	6	46	Endometrium	Endometrioid	1a	0	1
7	7	42	Endometrium	Endometrioid	1a	1	1
8	8	45	Endometrium	Endometrioid	1a	0	1
9	9	45	Ovary	Endometrioid	1b	-	2
10	10	46	Isthmus	Endometrioid	2	0	2
11	11	67	Endometrium	Endometrioid	1a	0	1
12	12	46	Endometrium	Endometrioid	1a	0	2
13	13	64	Endometrium	Endometrioid	1a	0	1
14	14	46	Endometrium	Endometrioid	1a	0	1
15	15	48	Endometrium	Endometrioid	1a	0	1
16	16	63	Endometrium	Endometrioid	1a	0	2
17	17	63	Endometrium	Endometrioid	1a	-	2
18	18	31	Endometrium	Mixed	1b	1	3
19	19 C	33	Endocervix	Endometrioid	1b	2	2
	19 E	33	Endometrium	Endometrioid	1a	1	3
20	20	42	Ovary	Carcinosarcoma	1c	0	3
21	21	54	Endometrium	Endometrioid	-	-	-
22	22	62	Endometrium	Undifferentiated	-	-	3
23	23	42	Endometrium	Endometrioid	1a	0	2
24	24	58	Endometrium	Endometrioid	-	-	3
25	25	55	Endometrium	Endometrioid	1a	0	2
26	26	51	Endometrium	Endometrioid	1b	X	1
27	27	37	Isthmus	Endometrioid	-	0	2
28	28	34	Endometrium	Mixed	2	0	2
29	29 O	41	Ovary	Endometrioid	1a	0	2
	29 I	41	Isthmus	Endometrioid	-	-	3
30	30	49	Ovary	Endometrioid	-	0	2
31	31	53	Endometrium	Endometrioid	1a	0	1
32	32	52	Ovary	Mixed	2	-	2
33	33	40	Ovary	Mixed	-	-	3
34	34	46	Isthmus	Endometrioid	-	-	-
35	35	60	Endometrium	Mixed	1a	0	3
36	36	54	Endometrium	Endometrioid	-	-	2
37	37	37	Endometrium	Mixed	-	-	3
38	38	45	Endometrium	Endometrioid	1b	0	1
39	39	65	Endometrium	Undifferentiated	-	-	3
40	40	61	Endometrium	Endometrioid	1a	0	2
41	41	56	Endometrium	Endometrioid	1a	-	1
42	42	69	Endometrium	Endometrioid	1a	0	2
43	43	54	Endometrium	Endometrioid	1a	-	2
44	44	56	Endometrium	Endometrioid	-	-	3
45	45	53	Ovary	Mixed	2b	0	2
46	46 E	44	Endometrium	Endometrioid	1a	0	1
	46 O	45	Ovary	Mucinous	1a	0	1
47	47	64	Endometrium	Endometrioid	1a	0	1
48	48	71	Endometrium	Endometrioid	1a	0	2
49	49	54	Endometrium	Endometrioid	1b	0	3
50	50	64	Endometrium	Endometrioid	1a	0	3

51	51	54	**Endometrium**	Clear Cell	1a	0	3
52	52	75	**Endometrium**	Clear Cell	1a	0	3
53	53	62	**Endometrium**	Endometrioid	1a	0	1
54	54	27	**Endometrium**	Endometrioid	-	0	2
55	55	71	**Endometrium**	Endometrioid	1a	0	2
56	56	68	**Endometrium**	Endometrioid	3a	0	2
57	57	35	**Endometrium**	Endometrioid	1a	0	1
58	58	41	**Endometrium**	Endometrioid	1a	0	1
59	59 E	48	**Endometrium**	Endometrioid	1a	0	1
	59 O	48	**Ovary**	Endometrioid	1a	0	1
60	60	43	**Ovary**	Endometrioid	1a	0	2
61	61	56	**Endometrium**	Endometrioid	1a	0	1
62	62	67	**Endometrium**	Endometrioid	1a	0	2
63	63	55	**Endometrium**	Endometrioid	1b	0	2
64	64	41	**Endocervix**	Endometrioid	1b1	0	1
65	65	57	**Endometrium**	Endometrioid	1a	0	2
66	66	41	**Endocervix**	Serous	1b	0	3
67	67	57	**Endometrium**	Endometrioid	1a	0	1
68	68	44	**Ovary**	Endometrioid	2b	0	3
69	69	29	**Ovary**	Endometrioid	-	-	2
70	70	52	**Endometrium**	Endometrioid	2	0	2
71	71	60	**Endometrium**	Endometrioid	1a	-	1
72	72	70	**Endometrium**	Endometrioid	1a	0	2
73	73	57	**Endometrium**	Mixed	-	1	3
74	74	72	**Endometrium**	Endometrioid	1a	0	2
75	75	53	**Endometrium**	Endometrioid	1a	-	1
76	76	56	**Endometrium**	Endometrioid	1a	0	1

Legend: **Endometrium**= corpus/fundus of the uterus; **Isthmus**= isthmus of the uterus

2. DNA extraction

Tumor DNA was obtained from formalin fixed and paraffin embedded (FFPE) tissues using three representative 8µm sections. The sections of every specimen were treated twice with Bio-Clear® (Bio-optica, Milan, Italy) and then rehydrated with a descending scale of ethanol. DNA was extracted using a QIAamp® DNA FFPE Tissue kit (Qiagen, Hilden, Germany) according to the manufacturer's protocol. Neoplastic areas were manually microdissected for DNA extraction and contained at least 35% of tumor cells, to minimize contamination by normal cell (Figure 4).

Each DNA was quantified using Qubit® dsDNA High Sensitivity (HS) Assay kit and Qubit® 2.0 Fluorometer (Invitrogen™, Thermo Fisher Scientific, USA).

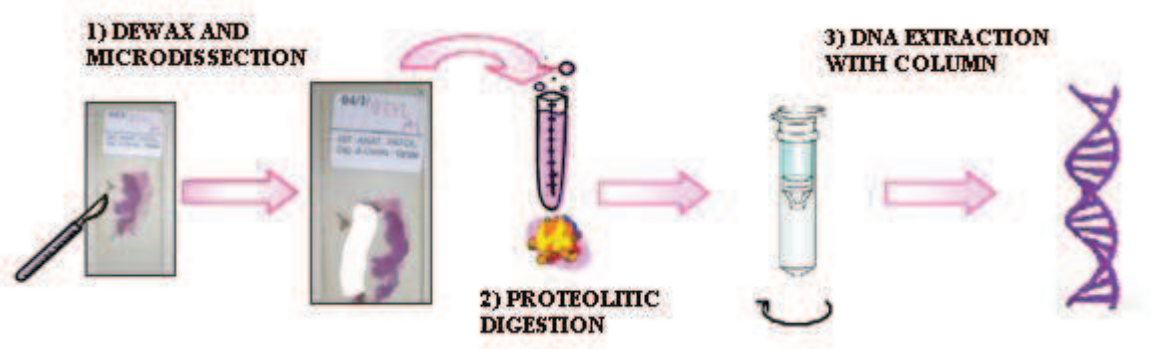

Figure 4. Manual microdissection and DNA extraction with column.

3. Immunohistochemical analysis

The immunohistochemical analysis was performed on 3μm sections of FFPE tissue using the monoclonal antibody listed in Table 3. The sections were dewaxed and rehydrated as previously described for DNA extraction and subsequently they were treated with 3% H_2O_2 solution for 10 minutes, in order to inhibit the endogenous peroxidase. The slides were heated in a microwave at 720 Watt for 4 cycles of 5 minutes submersed in citrate buffer at pH 6.0, in order to expose the antigen.

Staining was visualized by EXPOSE Mouse and Rabbit Specific HRP/DAB detection IHC kit (Abicam®, UK) or Ultravision™ Quanto Detection System HRP (Thermo Fisher Scientific, USA) and DAB staining. The sections were briefly colored with hematoxylin, dehydrated and, finally, assembled with the coverlids using PER-TEK Mounting Medium (Kaltek srl, Italy).

The samples were considered negative for the protein expression when the nuclear positivity was observed only in the internal control (stromal cells, muscular cells, normal epithelial cells or lymphocytes), but it was not observed in the cancer cell nuclei.

Table 3. Monoclonal antibody used for IHC analysis.

Antibody	Clone	Target	Dilution	Company
MLH1	G168-15	Whole protein	1/100	BD Pharmigen, USA
MSH2	FE-11	C-terminal fragment	1/200	Oncogene Research, USA
MSH6	44	Whole protein	1/200	Transduction Laboratories USA
PMS2	A16-4	C-terminal fragment	1/200	BD Pharmigen, USA
ARID1A	D2A8U	Whole protein	1/400	Cell Signaling Technology, USA

4. Microsatellite instability analysis by mononucleotide repeats pentaplex (MRP)

The microsatellite instability analysis was performed using a pentaplex panel of monomorphic mononucleotide repeats (NR21, BAT26, BAT25, NR24, NR22; Table 4) suggested by Suraweera et al [68]. The PCR reaction mix and the thermic profile are reported below (Table 5). The PCR fluorescent products were subjected to fragment analysis by automated sequencing (ABI PRISM 310, ThermoFisher scientific, USA) and analyzed with GeneMapper 4.0. (ThermoFisher Scientific, USA).

A tumor was considered microsatellite unstable (MSI) when at least two microsatellite loci were unstable, showing insertion/deletion of at least 3bp (Figure 5). Moreover, to correctly define the microsatellite status for each case we evaluated the electropherogram shape of each locus [76] which was defined as "Gaussian" shape (Figure 6A) in typical MSS cases or "non-Gaussian" shape when a biphasic (B), a left- or a right-tailed shapes (C and D) were observed in MSI cases. Those cases that did not fulfill MSS or MSI criteria were classified as "borderline" cases (B-MSI) and further described in Results section (Figure 6).

Table 4. Position, amplicon size, fluorescent labelling and primer sequence of mononucleotide repeats pentaplex (MRP).

Locus	Position	Amplicon size (bp)	Fluorescent labelling	Primer
NR-21	14q11.2	104	HEX	For: TAAATGTATGTCTCCCCTGG Back: ATTCCTACTCCGCATTCACA
BAT-26	2p21	116	6-FAM	For: TGACTACTTTTGACTTCAGCC Back: AACCATTCAACATTTTTAACCC
BAT-25	4q12	120	TET	For: TCGCCTCCAAGAATGTAAGT Back: TCTGCATTTTAACTATGGCTC
NR-24	2q11.2	130	HEX	For: CCATTGCTGAATTTTACCTC Back: ATTGTGCCATTGCATTCCAA
NR-22	11q24-25	141	6-FAM	For: GAGGCTTGTCAAGGACATAA Back: AATTCGGATGCCATCCAGTT

Table 5. Microsatellite pentaplex reaction mix and thermic profile.

Reaction mix	
Primer For	0.3 µM
Primer Back	0.3 µM
dNTPs	200 µM
MgCl2	2 mM
GoTaq Promega	2 units
Buffer 10X	1X
Final volume	15 µl

94°C	5'	
94°C	50"	
55°C	50"	X 10
72°C	50"	
89°C	30"	
55°C	30"	X 20
72°C	30"	
72°C	10'	

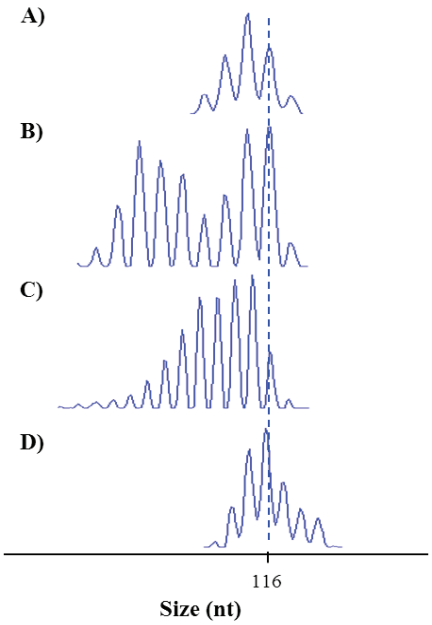

Figure 5. Shape of a repeat's plot (BAT26). A) MSS Gaussian shape; B) biphasic MSI aberrant shape; C) and D) examples of one tail MSI aberrant shape.

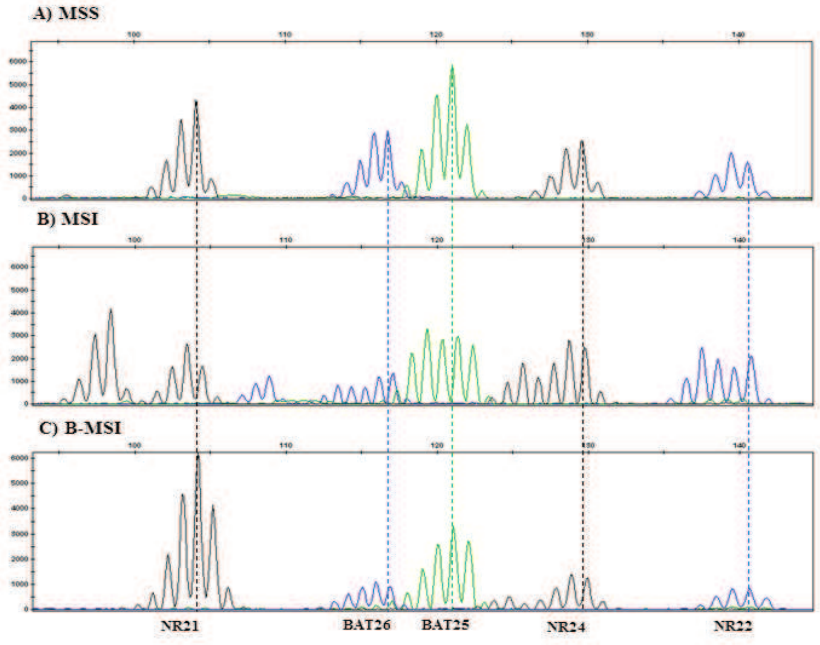

Figure 6. MSI analysis results of three illustrative cases. A) a microsatellite stable case, no shortenings or expansions are reported; B) a microsatellite unstable case with shortenings greater than 3bp; C) a borderline microsatellite unstable case characterized by the NR24 locus clearly unstable and the other four loci with shortenings lower than 3bp. The dotted lines indicate the expected size of each locus. *Legend:* MSS=microsatellite stable, MSI=microsatellite unstable, B-MSI= borderline microsatellite instability

5. Microsatellite instability analysis of nine additional loci

After a critical analysis of the literature, we selected nine loci of mononucleotide repeats in the coding sequence of seven genes that were altered in at least 25% of MSI GC cohorts [70-73]. For each locus, the type of repeats, primer sequences and PCR profiles are reported in Table 6, while the reagents and the reaction mix were the same used for MRP test. Aliquots of 0.3µl of the PCR fluorescent products were combined with 0.5µl TAMRA internal size standard (Applied Biosystems, Foster City, USA) and 16.5ul of deionized formamide. After denaturation, fragments were separated by electrophoresis on an ABI 310 capillary sequencer sequencing (ABI PRISM 310, ThermoFisher scientific, Waltham, USA) and analyzed with GeneMapper 4.0. Results were confirmed by direct sequencing using the same non-fluorescent primers and BigDye Terminator v1.1 (ThermoFisher scientific, Waltham, USA) as previously published by Carnevali et al [77]. A locus was scored as unstable when a deletion/insertion of at least one nucleotide was observed.

Table 6. List of the additional microsatellite loci.

Name	NCBI Reference Sequence	Length and location of the repeats	Primer sequence 5' to 3'	PCR profile	PCR product size (bp)
RPL22	NM_000983	A8, exon 2	ggagcacacttccgttagtt ggtgggtgcaatcaagagtg	TD: 70°C-62°C	148
SRPR	NM_003139	A8, exon 4	tccatgattgagacacgggg accacctcagtccttagcac	TM: 56°C	145
MBD6_1	NM_052897	C7, exon 7	ccaagtggggagccattttc gccagcagcgcagaatttaa	TM: 56°C	104
MBD6_2	NM_052897	C7, exon 7	gctttaaattctgcgctgctg tgattcccagctcccatctc	TD: 68°C-65°C	126
MBD6_3	NM_052897	C7, exon 8	cacctacctccagtgtcacc cacactccctcagactcacc	TD: 68°C-60°C	149
NRIP1	NM_003489	A8, exon 3	tgtcctccagttgctcctg tctctctgagtgttcctgagt	TD: 63°C-55°C	100
JAK1	NM_002227	A8, exon 5	agtgtggcgtcattctcca tgagcaaacagatactccagtg	TD: 68°C-62°C	108
JMJD1C	NM_004241	A8, exon 9	ccagaatcccagtcaccact actcctctcacacatgcctag	TD: 64°C-56°C	109
SVIL	NM_003174	G7, exon 31	cgcgcccctacctatttac ttcttcttcctcttcccgcc	TD: 68°C-62°C	134

Legend: TD=Touch-Down PCR, TM=Melting Temperature, bp=base pair

6. MLH1 promoter methylation analysis using MS-MLPA

The SALSA MS-MLPA ME011 Mismatch Repair genes (MMR) Kit (MRC-Holland, Amsterdam, The Netherlands) was used to perform *MLH1* promoter methylation analysis on IHC MLH1 negative tumor.

This ME011 Mismatch Repair genes probemix was developed to detect aberrant CpG island methylation of several MMR genes and included six probes for *MLH1* (3p22.1), six probes specific for the *MGMT* promoter region (10q26), four probes for *MSH2* (2p21), three probes for *MSH6* (2p16), three probes for *PMS2* (7p22), two probes for *MSH3* (5q14.1), and one probe for *MLH3* (14q24.3). The most important methylation region for *MLH1* expression, the Deng C-region, is from -248 nt to -178 nt before the transcription start site and the second most important region, the Deng D-region, is from -9 nt to +15 nt (Figure 7) [28, 29]. Additional information, such as probe sequences and chromosomal locations can be found at www.mlpa.com.

All MS-MLPA reactions were done according to the manufacturer's instructions, using 100-150ng of DNA. The probemix is added to 5µl of denatured DNA and allowed to hybridize for 16 hours at 60°C. Subsequently, the sample is divided in two: one half is ligated by adding 10µl of ligase-mix, whereas in the other half ligation is combined with digestion by adding 10µl of ligation-digestion mix. These samples are incubated for 30 minutes at 54°C, then the HhaI enzyme is inactivated by denaturation at 95°C for one minute. Since the unmethylated sequences are cut by the restriction enzyme, this process results in the ligation of the methylated sequences only. Eight microliters of the two aliquots are then amplified in a 25µl PCR reaction using Veriti thermocycler (Applied Biosystems, Foster City, USA) with the following thermal protocol: 33 cycles of denaturation at 95°C for 20 seconds, annealing at 60°C for 30 seconds and extension at 72°C for 1 minute with a final extension of 20 minute at 72°C. In order to assess MS-MLPA reliability two replicates were performed for each sample and positive and negative controls using fully methylated DNA (CpGenome Universal Methylated DNA, Millipore) and unmethylated DNA (CpGenome Universal UnMethylated DNA, Millipore) were included in each MS-MLPA experiment. Aliquots of 1.5µl of the PCR reaction were combined with 0.5µl TAMRA internal size standard (Applied Biosystems, Foster City, USA) and 13.5µl of deionized formamide. After denaturation, fragments were separated and quantified by electrophoresis on an ABI 310 capillary sequencer and analyzed with

GeneMapper 4.0. (Applied Biosystems). Values corresponding to peak size (base pairs) and peak height were used for further data processing by Coffalyser V7 software (MRC-Holland).

Methylation dosage ratio (MR) was obtained by the following calculation: MR= (Px/Pctrl)Dig / (Px/Pctrl)Undig where Px is the peak height of a given probe, Pctrl is the sum of the peak heights of all control probes, Dig stands for HhaI digested sample, and Undig stands for undigested sample.

A methylation ratio (MR) for a given gene may range from 0 (0% of alleles methylated) to 1.0 (100% of alleles methylated) and threshold values of 0.3 and 0.7 are suggested by the manufacturer to consider a locus as hemi-methylated or fully-methylated, respectively.

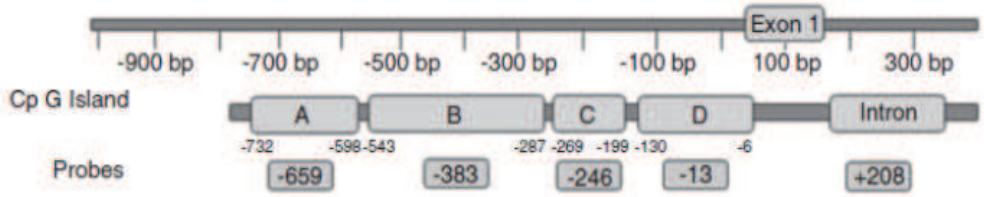

Length (nt)	SALSA MLPA probe	Gene	HhaI site	Ligation site (Distance to ATG start)	Partial sequence with HhaI site	Distance to next probe
237	7187-L7710	MLH1	+	- 659 (Deng, A-region)	TCCGCCACATACCGCTCGTAGTAT-TCGTGCTCAGCCTCGTAGTGGCGCCTGAC	0.1 kb
148	1685-L1265	MLH1	-	- 518 (Deng, B-region)	GGGTCCACTCGGGCCGGAAAACT-AGAGCCTCGTCGACTTCCATCTTGCTTCTTT	0.1 kb
265*	6221-L1747	MLH1	+	- 383 Reverse (Deng, B-region)	CTGCTGAGGTGATCTGGCGCAGA-GCGGAGGAGGTGCTTGGCGCTTCTCAGGC	0.1 kb
198	6222-L7712	MLH1	+	- 246 (Deng, C-region)	AGAGCGGACAGCGATCTCTAACGCGCAA-GCGCATATCCTTCTAGGTAGCGGGCAGTA	0.2 kb
166	1686-L1266	MLH1	+	- 13 (Deng, D-region)	CGTTGAGCATCTAGACGTTTCCTTGGCTCT-TCTGGCGCCAAAATGTCGTTCGTGGCAGG	0.2 kb
292	2258-L1745	MLH1	+	+ 208 (Intron 1, 93 nt after exon 1)	CGGACACGCCTCTTTGCCCGGGCAGA-GGCATGTACAGCGCATGCCCACAACGGCG	

Figure 7. Representation of *MLH1* promoter region and list of MS-MLPA probes (ME-011 MRC-Holland, Amsterdam, The Netherlands)

7. Validation of MS-MLPA results by bisulphite-pyrosequencing

To validate the MS-MLPA results, bisulphite pyrosequencing was used to confirm methylation patterns of the *MLH1* gene. Bisulfite modification of genomic DNA (300 ng) was performed with an EpiTect Bisulfite Kit (Qiagen, Hilden, Germany) according to the manufacturer's recommendations. Bisulfite-modified DNA was amplified and sequenced by using primers and protocol reported below (Table 7 and 8).

Pyrosequencing was carried out with PyroGold reagents on a PyroMark Q96 ID system (Qiagen, Hilden, Germany). Pyrogram outputs were analyzed by the Pyromark Q24 software using the Allele Quantification software (Qiagen, Hilden, Germany) to determine the percentage of methylated alleles at each CpG site examined. Presence of MLH1 promoter methylation was scored when the mean value of the percentage of methylated alleles was higher than 15%.

Table 7. Primer sequence of *MLH1* methylation PCR.

Primer	Sequence
MLH1 For	GAGTTTTTAAAAAAGAATTAATAGGAAGAG
MLH1 Back	ATACTACCCCCTACCTAAAAAAATAT
MLH1 Seq	CTACCCCCTACCTAAAAAAATATAC

Table 8. Reaction mix and thermic profile of *MLH1* methylation PCR

Reaction mix	
Primer For	0.4 µM
Primer Back	0.4 µM
dNTPs	200 µM
MgCl2	2 mM
Epitaq Takara	2 units
Buffer 10X	1X
Final volume	50 µl

95°C	2'	
95°C	25''	
57°C	30''	X 35
72°C	30''	
72°C	5'	

8. Selection of 16 genes involved in endometrial cancer development for NGS analysis

In order to further characterize the molecular profiles of endometrial cancers of our cohort, we decided to study 16 genes involved in endometrial carcinogenesis through genetic and epigenetic mechanisms with MiSeq technology (Illumina, San Diego, California, USA).

First, we identified in literature 16 candidate genes which were reported to be associated to endometrial cancer [6, 78-82] and we evaluated the frequency of mutation in endometrial cancer for each gene using COSMIC website (Catalogue of somatic mutations in cancer, http://cancer.sanger.ac.uk/cosmic, Table 9). Subsequently, we designed a custom panel for exon sequencing of these genes using GeneRead DNAseq Mix-n-Match Panel (Qiagen), defining 150bp as amplicon size (ideal for low-quality fragmented DNA, such as FFPE DNA) and choosing 10 exon flanking bases to cover the exon/intron junctions (Figure 8, https://www.qiagen.com/it/shop/genes-and-pathways/custom-products/custom-array-products/generead-designer/).

Table 9. 16 genes studied with MiSeq.

Gene	position	% mutations COSMIC	Protein family	Function
MLH1	3p22.2	2%.	Mismatch Repair	DNA mismatch repair. DNA damage signaling
MSH2	2p21	2.18%	Mismatch Repair	DNA mismatch repair. DNA homologous recombination repair.
MSH6	2p16.3	5.48%	Mismatch Repair	DNA mismatch repair. DNA homologous recombination repair.
MSH3	5q14.1	1.41%	Mismatch Repair	DNA mismatch repair.
MLH3	14q24.3	3.13%	Mismatch Repair	DNA mismatch repair.
TP53	17p13.1	18.63%	Cell cycle regulator	Growth arrest or apoptosis.
PTEN	10q23.3	37.69%	Phosphatase	Modulator of the AKT-mTOR signaling pathway. Antagonizes the PI3K-AKT/PKB signaling pathway
PIK3CA	3q26.3	23%	PI 3-Kinases	Role in cellular signaling in response to growth factors.
CTNNB1	3p22.1	17.55%	Adherent junctions	Key downstream component of Wnt signaling pathway. Regulation of cell adhesion
KRAS	12p21.1	14.8%	RAS gene	Role in the regulation of cell proliferation; role in promoting oncogenic events.
POLE	12q24.3	6.45%	Polymerase ε	Catalytic subunit of DNA polymerase epsilon, DNA repair activity.
POLD1	19q13.3	2.19%	Polymerase δ	Catalytic subunit of DNA polymerase delta, exonucleolytic activity.
ARID1A	1p36.1	24.65%	BAF chromatin-remodeling complex, SWI/SNF	Transcriptional activation and repression of select genes by chromatin remodeling (alteration of DNA-nucleosome topology).
ARID2	12q12	2.97%	BAF chromatin-remodeling complex, SWI/SNF	Transcriptional activation and repression of select genes by chromatin remodeling (alteration of DNA-nucleosome topology).
SMARCA4	19p13.2	3.59%	SWI/SNF	Transcriptional coactivator cooperating with nuclear hormone receptors to potentiate transcriptional activation.
EZH2	7q36.1	2.19%	Polycomb-group (PcG)	Maintaining the transcriptional repressive state of genes over successive cell generations.

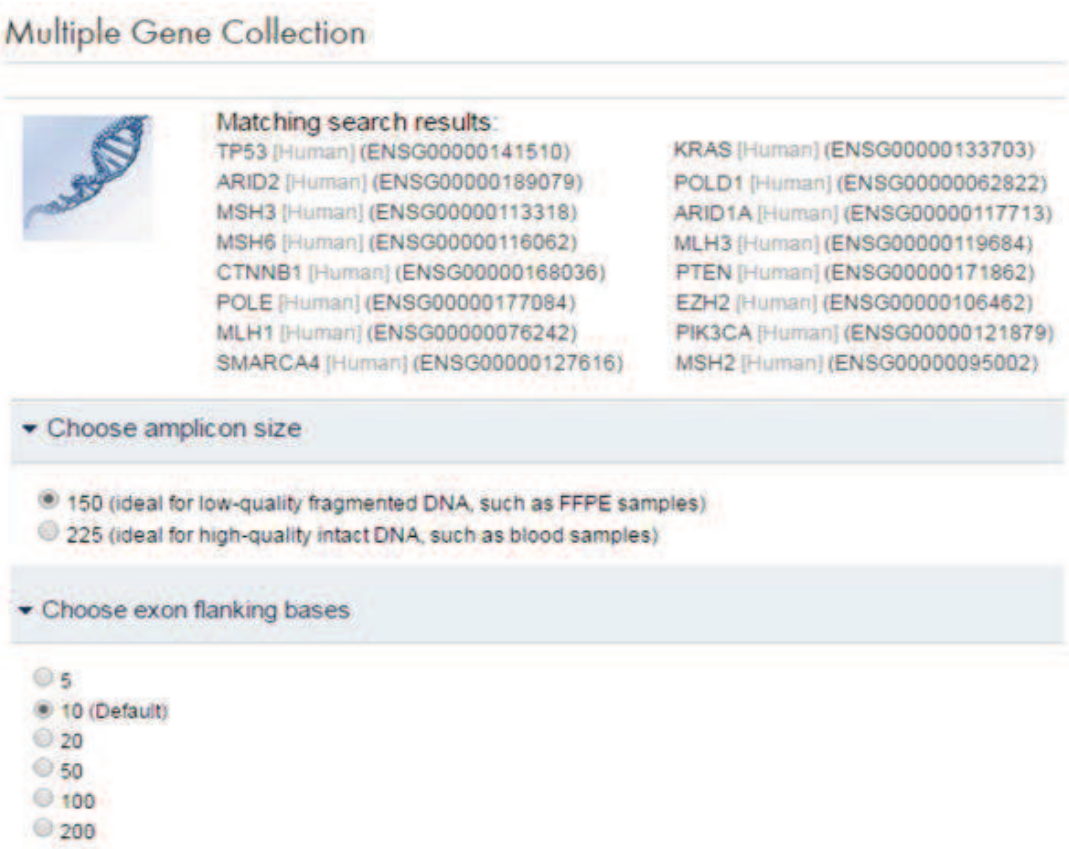

Figure 8. Detailed flowchart for a custom panel design.

9. Targeted gene sequencing with MiSeq

A subset of 35 endometrial cancers of our cohort was tested with the previously selected gene panel in collaboration with Sergio Marchini's laboratory at "Mario Negri" Institute for Pharmacological Research (Figure 9) [83]. Since high-quality DNA is essential for obtaining good sequencing results, tumor DNA (35 tumor samples) and normal DNA for comparison (35 normal samples) were extracted using Maxwell 16 system (Promega, Madison, Wisconsin, USA) according to the manufacturer's protocol in our laboratory. Sample quality control (Sample QC) was performed using a real-time PCR assay, Infinum FFPE QC kit (Illumina, USA). The samples that passed the quality control underwent to a target enrichment of the 16 genes using a PCR approach and four pools of primers as reported in GeneRead DNAseq Targeted Panels V2 Handbook (Qiagen, Hilden, Germany). After the PCR purification using AMPure XP beads and a quality control step performed with Agilent 2100 Bioanalyzer (Agilent Technologies), we proceeded with the library construction using GeneRead Library I Core Kit and GeneRead Adapter I Set A and B (Qiagen, Hilden, Germany) as shown in GeneRead DNAseq Targeted Panels V2 Handbook. Briefly, the PCR-enriched DNA was cut with an end-repair enzyme, then, after a single adenine addition to the DNA ends, a barcode adapter was ligated to the DNA. Each sample was tagged with a specific barcode, in order to sequence up to 24 samples in a single run. After cleanup of adapter-ligated DNA with AMPure XP beads, the libraries were amplified using GeneRead DNA I Amp Kit (Qiagen, Hilden, Germany) according to GeneRead DNAseq Targeted Panels V2 Handbook. The amplified libraries were cleanup with AMPure XP beads and a quality control step was performed using Agilent 2100 Bioanalyzer (Agilent Technologies). In the end, 24 libraries were pooled together, loaded in a single V2 flow cell and sequenced using MiSeq system.

Raw de-multiplexed reads were first aligned to the reference human genome (UCSC build hg19) using the Burrows-Wheeler Aligner (BWA). Somatic variant calls were detected using two different variant caller, MuTect2 and Vardict. Each sample was matched with its normal tissue. Then, data were filtered with a coverage of at least 200X and an allelic fraction of at least 5% according to NGS analysis on FFPE samples [84-87]. Both synonymous mutations outside the splicing regions and variants described in the 1000 Genome Project were filtered out.

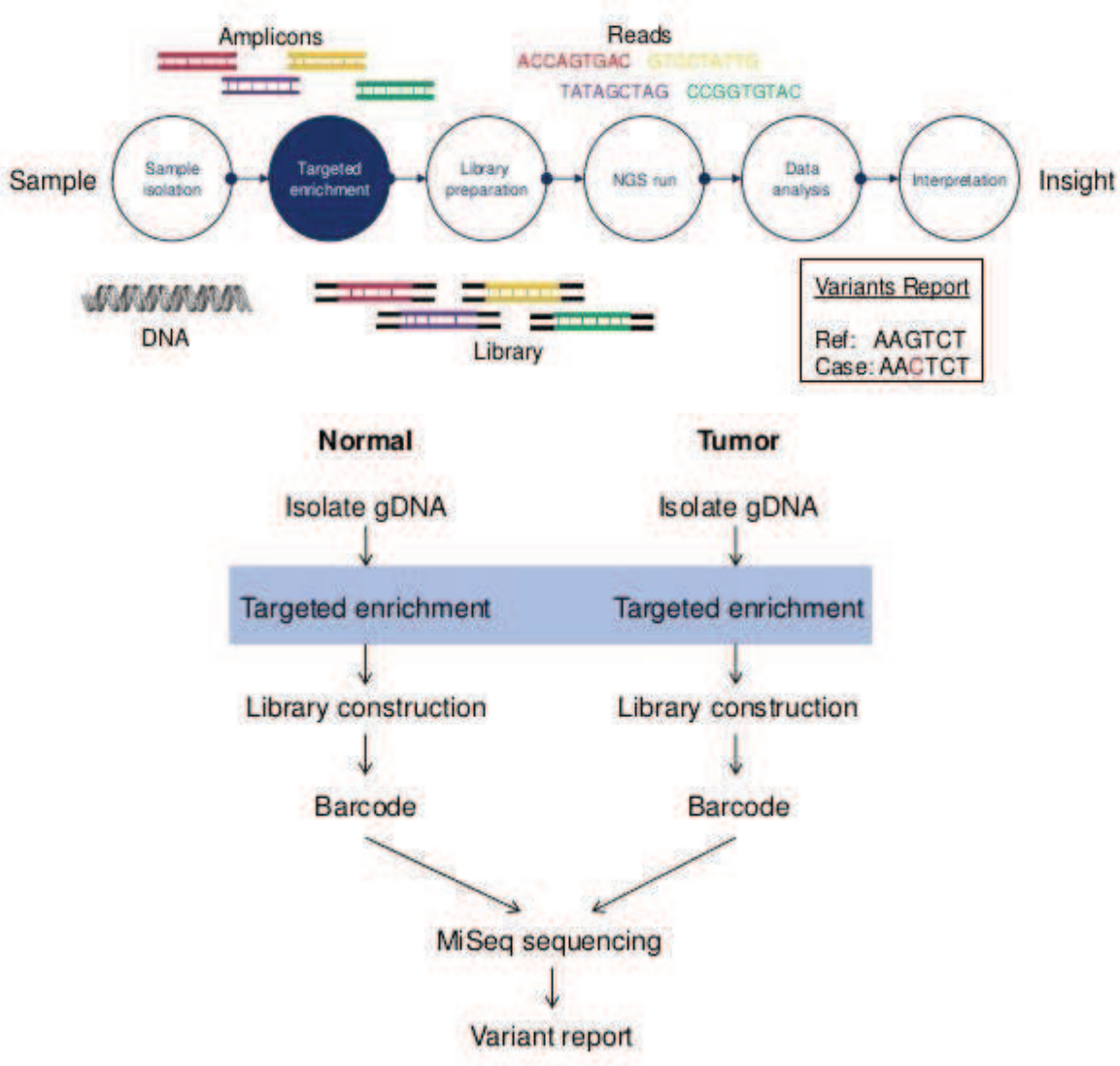

Figure 9. GeneRead DNAseq Targeted Panels V2 workflow (Qiagen, Hilden, Germany)

10. Statistical analysis

The statistical analysis was performed using Graph Pad PRISM v.5. Univariate comparisons of continuous data were carried out using Student's t-test and discrete variables were compared with $\chi 2$ test or Fisher's exact test. All comparisons were two-sided and a p-value <0.05 was considered to be significant.

RESULTS

1. MMR–DEFICIENCY ANALYSIS

1.1 Immunohistochemical evaluation of MMR proteins

The immunohistochemical analysis of four MMR proteins (MLH1, MSH2, MSH6 and PMS2) was performed in our series. An example of loss of expression of MLH1/PMS2 proteins is reported in Figure 10. As shown in Supplementary Table 1, we observed a normal expression of MMR proteins in 22 out of 80 GCs (27.5%, MMR proficient group, p-MMR) while the remaining 58 GCs showed the loss of expression of at least one MMR protein (72.5%, MMR deficient group, d-MMR). As shown in Table 10, the p-MMR group was composed by 17 endometrial, two endocervical and three ovarian carcinomas, while the d-MMR group included 43 endometrial (corpus and fundus), two endocervical, nine ovarian carcinomas and four cancers of the isthmus. In the majority of d-MMR cases, we observed the combined loss of both eteroduplex proteins (MLH1/PMS2 or MSH2/MSH6, Figure 11). We observed the IHC loss of expression of MLH1/PMS2 eteroduplex in 25 cases (43%), MSH2/MSH6 eteroduplex in 24 cases (41%), MSH6-only in eight cases (14%) and PMS2-only in one case (2%). Interestingly, case#55 showed a focal MLH1/PMS2 loss of staining in the 60% of the tumor cells, while the remaining 40% showed a normal IHC staining of all MMR proteins (Supplementary Table 1).

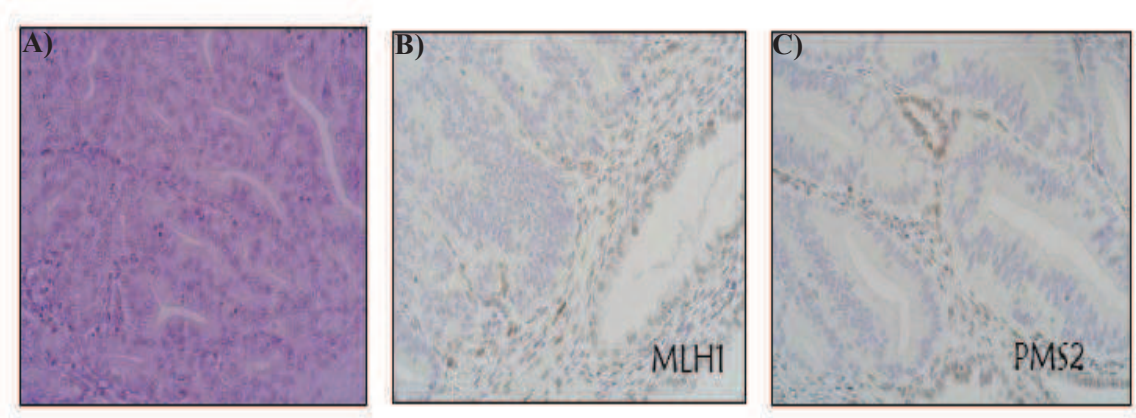

Figure 10. Example of an endometrioid endometrial cancer (hematoxylin-eosin staining, A) with loss of IHC expression of MLH1 (B) and PMS2 (C) proteins.

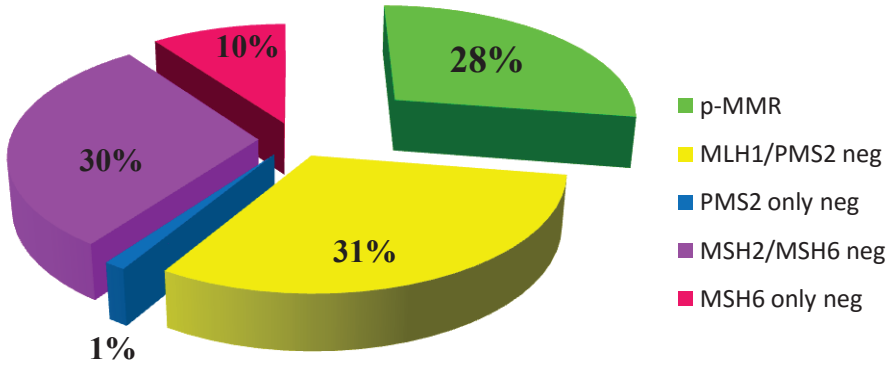

Figure 11. Frequencies of different MMR immunophenotypes in the 80 gynecological cancers examined

Table 10. Tumor sites and expression of MMR proteins.

	MMR PROFICIENT (22 GC, 28%)	MMR DEFICIENT (58 GC, 72%)
Site		
Endometrium (60)	17	43
Isthmus (4)	-	4
Endocervix (4)	2	2
Ovary (12)	3	9

Legend: MMR=mismatch repair, GC=gynecologic cancer

1.2 Microsatellite instability analysis by mononucleotide repeats pentaplex (MRP)

We evaluated MSI status of 22 p-MMR and 58 d-MMR GCs using MRP. Twenty-one out of 22 p-MMR GCs were classified as MSS: 19 cases did not show any alteration and two cases showed 1bp deletion at BAT25 locus. Unexpectedly, one p-MMR GC showed a MSI profile with shortenings greater than 3bp in NR-21, BAT-25 loci and a non-Gaussian repeats shape (case#40, discordant case).

MRP analysis of 58 d-MMR GCs identified 43 cases with MSI profile, nine B-MSI GCs and six GCs with MSS profile (Figure 12).

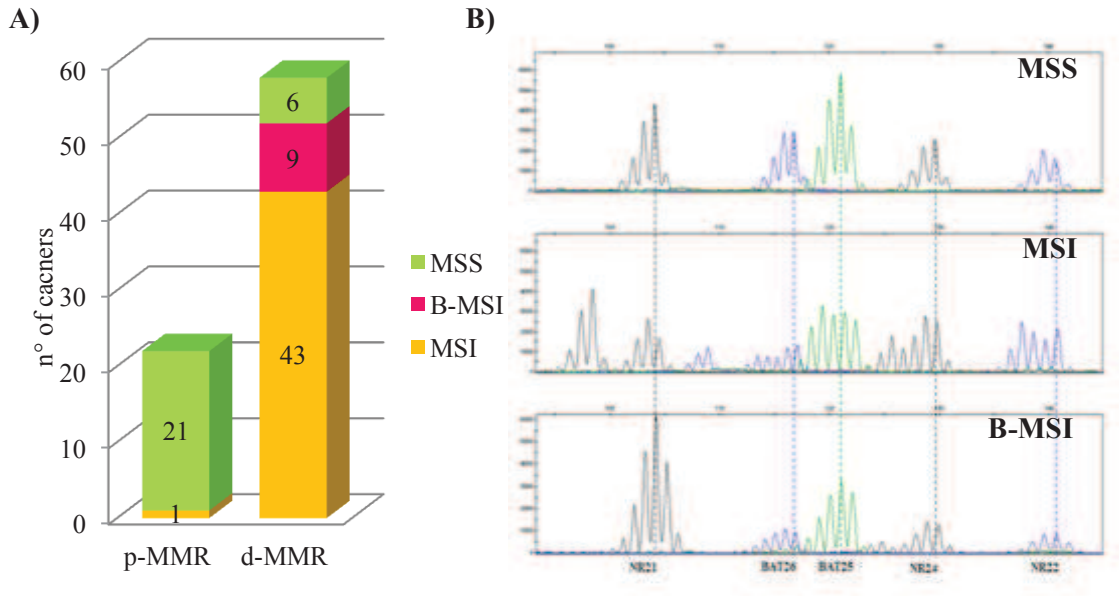

Figure 12. MRP MSI analysis of 80 gynecological cancers. A) Distribution of MSI, B-MSI and MSS cases in p-MMR and d-MMR groups. B) Three representative examples of MSS, MSI and B-MSI using MRP test.

The immunohistochemical study of MSI cases revealed the loss of MLH1-PMS2 proteins in 19 cases, PMS2-only in one case, MSH2-MSH6 in 21 cases and MSH6-only in two cases.

As shown in Supplementary Table 1, six MMR deficient GCs fulfilled the criteria for MSS and were identified as discordant cases (case#38, 39, 43, 45, 54 and 55). Four cases (three uterine cancers and an ovarian one) were MLH1-PMS2 negative and two uterine cancers were MSH6-only negative.

B-MSI cases did not satisfy neither MSI nor MSS criteria as they showed insertion/deletion smaller than 3bp in at least two loci, although they were characterized by

a non-Gaussian repeats shape (case#9, 10, 11, 14, 20, 21, 32, 33 and 41). In detail, four GCs showed only one locus clearly unstable (i.e. with shortenings/expansions ≥3bp) and at least an additional locus with shortenings/expansions of one or two nucleotides. In the remaining five cases, two or more loci showed shortenings/expansions of one or two nucleotides. These cases included two endometrial cancers that were MLH1-PMS2 negative, three MSH2-MSH6 negative GCs (two ovarian and one uterine cancer) and four GCs (two ovarian and two uterine cancers) that were MSH6-only negative (Table 11).

Interestingly, while the MSI cases encompassed comparable percentages of MLH1-PMS2 negative and MSH2-MSH6 negative cases (20/43 cases and 23/43 cases, respectively), B-MSI was associated to the MSH2 and/or MSH6 eteroduplex deficit (7/9 cases), but the statistical significance was not reached probably due to the small size of this group of cases (p=0.3, Figure 13A). Moreover, B-MSI GC were found preferentially among ovarian cancers with respect to the other d-MMR cases (4/9 *versus* 5/50 cases, p=0.02, Figure 13B).

Finally, comparing the results from IHC and MRP analysis, we observed a global concordance of 91.3% (seven discordant cases: one p-MMR and six d-MMR).

Table 11. MMR proteins status and MRP analysis.

MMR protein status	MSS CASES (27 GC)	MSI CASES (44 GC)	B-MSI CASES (9GC)
MLH1/PMS2 neg	4*	19	2
PMS2 only neg	-	1	-
MSH2/MSH6 neg	-	21	3
MSH6 only neg	2*	2	4
No MMR loss	21	1*	-

Legend: MMR=mismatch repair, neg=negativity, GC=gynecologic cancer, MSS=microsatellite stable, MSI=microsatellite unstable, B-MSI=microsatellite borderline, *discordant cases

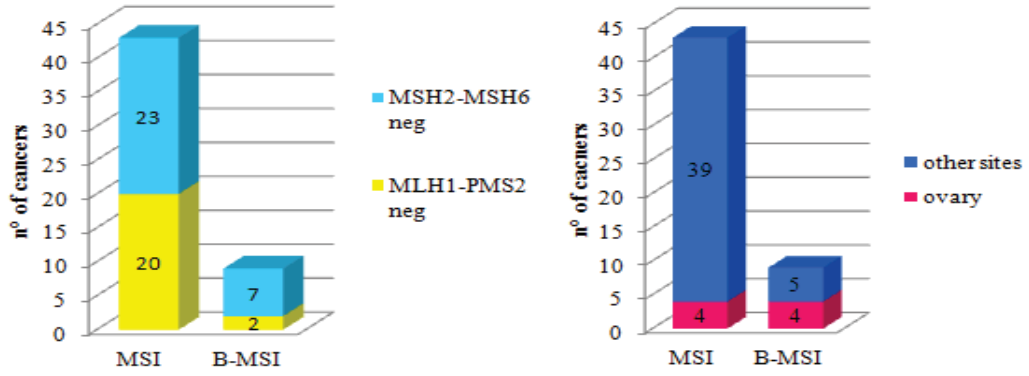

Figure 13. Distributions of MSI and B-MSI cases based on IHC results and tumor sites.

1.3 Microsatellite instability analysis of additional loci

We evaluated the status of nine additional microsatellite loci (Table 6) in the p-MMR (22 cases) and in 55 d-MMR cases by fragment analysis and Sanger sequencing validation; three d-MMR cases were not evaluable for this analysis (Supplementary Table 1, Figure 14). We never observed alterations in *SVIL*, *JAK1*, *JMJD1C* and in two loci of *MBD6* gene, thus these loci were excluded from further analyses. As reported in Figure 14, in 26 out of 55 d-MMR GC (47.3%) at least one of the remaining loci (*RPL22*, *SRPR*, *NRIP1* and *MBD6_3*) was unstable. Moreover, at least one of these loci was mutated in one p-MMR case (case#40, IHC-MRP discordant case) in agreement with MRP analysis.

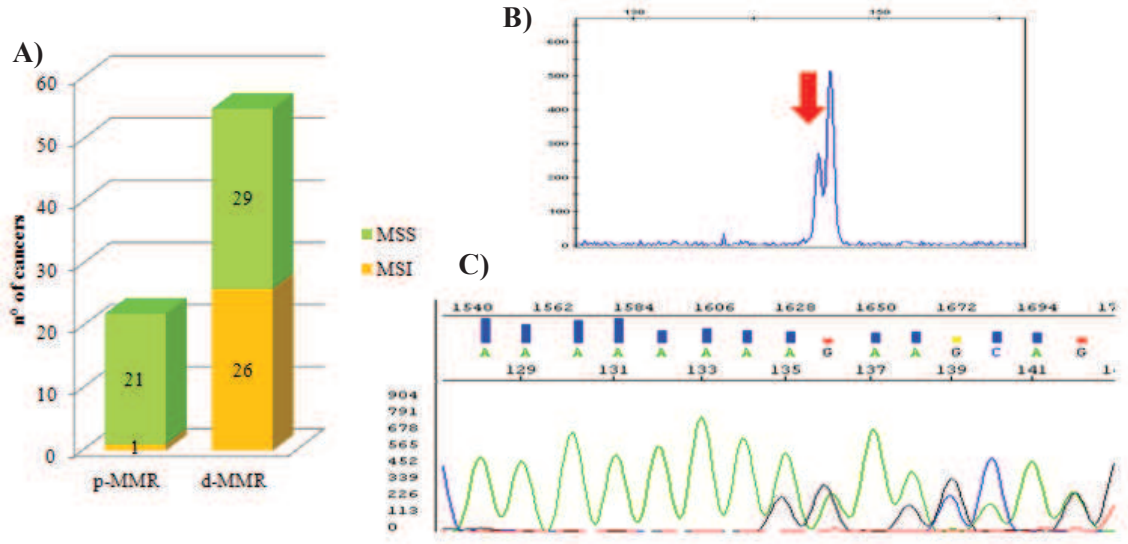

Figure 14. Additional loci MSI analysis of 77 gynecological cancers. A) Distribution of MSI (at least one additional locus mutated) and MSS cases in p-MMR and d-MMR groups. B) Representative *RPL22* instability by fragment analysis (case #40). C) Confirmation of *RPL22* instability by Sanger sequencing.

In detail, *RPL22* was mutated in 38.2% of d-MMR cases, followed by *SRPR* (16.4%), *NRIP1* (4%) and *MBD6_3* (2%). Overall, these additional loci had a lower concordance with IHC with respect to MRP analysis (61% vs 91.3%, Table 12). Notably, one case of six discordant d-MMR cases which resulted MSS by MRP test (case#55) and the only discordant p-MMR case (case#40, MSI without any MMR protein loss) showed instability at *RPL22* locus. This locus was strongly associated to MLH1-PMS2 defects as in this group 13 cases (54.1%) were *RPL22* unstable versus seven mutated cases in MSH2-MSH6 group (22.6%, p=0.023, Figure 15). Moreover, *RPL22* and/or *SRPR* were unstable in three out nine B-MSI GCs (33.3%), suggesting that these loci could be used to better characterize this subset of cancers. Using both MRP panel and these two additional loci,

we observed a global concordance with IHC analysis of 93.5% (72/77 cases evaluable with both methods).

Table 12. MMR proteins status and additional loci MSI analysis.

MMR protein status	MSS CASES (51 GC)	MSI* CASES (26 GC)
MLH1/PMS2 neg	8	15
PMS2 only neg	1	-
MSH2/MSH6 neg	14	9
MSH6 only neg	7	1
No MMR loss	21	1

Legend: MMR=mismatch repair, neg=negativity, GC=gynecologic cancer, MSS=microsatellite stable, MSI=microsatellite unstable, *at least an additional locus mutated

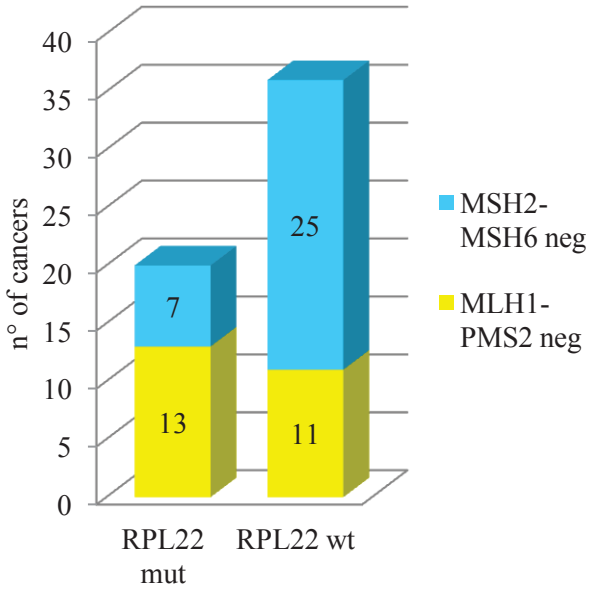

Figure 15. Distributions of *RPL22* mutated and wild-type cases based on IHC results.

2. HEREDITARY AND SPORADIC MMR DEFECT

In order to distinguish sporadic cases from Lynch syndrome patients, the germline mutational analysis and *MLH1* promoter methylation test were performed for those patients that displayed a cancer with MMR IHC loss of staining and/or MSI status (58 d-MMR GCs and one p-MMR GC, case #40), for a total of 56 patients (three patients showed double synchronous/metachronous cancers). All 56 patients who were tested for MMR germline analysis have previously signed an informative consent.

2.1 MMR germline mutation analysis

The germline analysis of *MLH1*, *MSH2*, *MSH6*, *PMS2* and *EPCAM* genes was performed at the Experimental Oncology laboratory (National Cancer Institute, CRO Aviano, Italy) directed by Dr. Alessandra Viel, using Sanger sequencing analysis for the detection of germline variants in the coding sequence or in the exon-intron junctions and MLPA assays (kit SALSA-P003 e SALSA P-284, MRC Holland) for the detection of large rearrangements of the genes. According to IARC (International Agency of Research on Cancer) classification, 26 out of 56 patients carried a pathogenic variant of a MMR gene (class 5, 46.4%), while 14 patients displayed a variant with uncertain significance (VUS, class 3, 25%) which segregates with disease. No germline variants were identified for 16 patients (28.6%, Supplementary Table 1).

Considering each single MMR gene, we identified nine *MLH1* germline variants (7 pathogenic variants and 2 VUS), 12 pathogenic *MSH2* variants, 17 *MSH6* variants (5 pathogenic variants and 12 VUS) and 2 pathogenic *PMS2* variants (Figure 16).

As shown in Supplementary Table 1, these mutations were 16 missense variants, seven frameshift variants, 12 variants in non coding regions (five in splice donor or acceptor sites and seven in UTR regions) and five large deletions (detected with MLPA analysis).

Interestingly, three out of seven patients with IHC/MSI discordant GCs (cases#38, 39 and 40) carried a *MSH6* or *MLH1* germline variant as shown in Supplementary Table 1.

The 16 patients, that did not display a MMR germline variant, were composed by 15 patients that harbored MLH1-PMS2 IHC negative GCs and one patient with MSH2-MSH6 negative cancer (case#44).

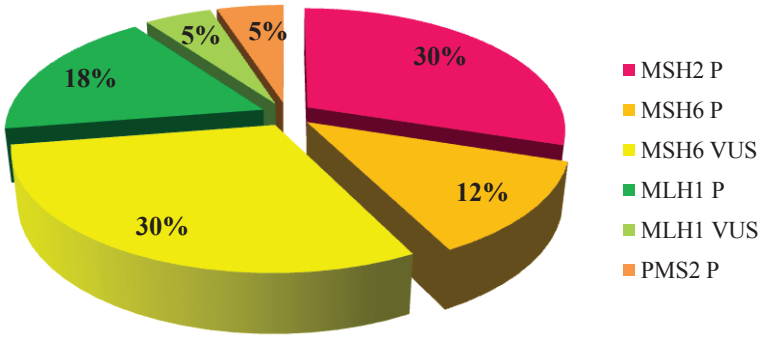

Figure 16. MMR germline variants frequencies. P=pathogenic variant (IARC class IV or V); VUS=variant with uncertain significance (IARC class III).

2.2 *MLH1* promoter methylation analysis

MLH1 promoter methylation analysis was performed using MS-MLPA on 24 GCs showing loss of MLH1 protein expression and on case#40, exhibiting MSI but no IHC loss of any MMR protein. Moreover, the MS-MLPA results were validated using bisulfite-pyrosequencing analysis of *MLH1* promoter methylation.

The results of this analysis are reported in Table 13: all samples that showed a methylation ratio (MR) greater than 0.3 in C, D and intron regions were considered methylated (M, in yellow). The samples showing a MR greater than 0.3 in A and B regions only were not considered methylated (U, unmethylated), because, as suggested by literature, the methylation of these two regions is not predictive for *MLH1* gene silencing [28, 29].

In detail, 14 GCs (12 endometrial and two ovarian cancers) showed methylation of all *MLH1* promoter regions, two cases exhibited methylation in A, B and C regions (case#5 and case#6). B and/or A region showed methylation in three samples (case#23, case#40, case#42) that were considered unmethylated. Interestingly, Case#55, which presented a clonal MLH1/PMS2 IHC negativity (in 60% of cancer cells) and MSS phenotype, showed an atypical methylation pattern with respect to the other cases. Indeed, C region in this sample showed low levels of methylation that were detected only by bisulfite-pyrosequencing but not by MS-MLPA analysis (Table 13).

Notably, in three out of seven IHC/MSI discordant cases (cases#45, 54 and 55) we observed *MLH1* promoter methylation as shown in Supplementary Table 1.

Table 13. MLH1 promoter methylation analysis.

P ID	T ID	Site	MSI	IHC	MLH1 METHYLATION							MMR germline variant (IARC classification)
					Somatic (MS-MLPA)					Somatic (PYRO)	Germline	
					A	B	C	D	In			
2	2	Ov	MSI	MLH1-PMS2 neg					U	U	-	*MLH1* (class 5)
3	3	End	MSI						U	U	-	*MLH1* (class 5)
4	4	Cerv	MSI						U	U	-	*MLH1* (class 5)
11	11	End	B-MSI						U	U	-	*MLH1* (class 3)
36	36	End	MSI						U	U	-	*MLH1* (class 3)
43	43	End	MSS						U	U	-	wt
42	42	End	MSI						U	U	-	wt
23	23	End	MSI						U	U	-	*PMS2* (class 5)
5	5	End	MSI						M	M	U	*MLH1* (class 5)
6	6	End	MSI						M	M	M	*MLH1* (class 5)
13	13	End	MSI						M	M	U	*MLH1* (class 5)
41	41	End	B-MSI						M	M	U	wt
45	45	Ov	MSS						M	M	-	wt
46	46 E	End	MSI						M	M	U	wt
	46 O	Ov	MSI						M	M		
47	47	End	MSI						M	M	U	wt
48	48	End	MSI						M	M	U	wt
49	49	End	MSI						M	M	U	wt
50	50	End	MSI						M	M	U	wt
51	51	End	MSI						M	M	U	wt
52	52	End	MSI						M	M	U	wt
53	53	End	MSI						M	M	U	wt
54	54	End	MSS						M	M	U	wt
56	56	End	MSI						M	M	U	wt
55	55	End	MSS						M	M	U	wt
40	40	End	MSI	p-MMR					U	U	-	*MLH1* (class 5)

Legend: P ID=patient ID, T ID=tumor ID, End=endometrium, Ov=ovary Cerv=endocervix, Isth=isthmus, yellow=methylated *MLH1* region, U=unmethylated, M=methylated, PRO/MSI=IHC proficient/microsatellite instable, IARC=International Agency for Research on Cancer, wt= no MMR germline variant (*MLH1*, *MSH2*, *MSH6* or *PMS2*)

2.3 *MLH1* promoter methylation and MMR germline mutations in sporadic and LS tumors

As shown in Table 13 and in Figure 17, among the nine *MLH1* promoter unmethylated GCs, five patients displayed a germline *MLH1* or a *PMS2* pathogenic variant, two cases presented a *MLH1* VUS and two cases did not display any MMR germline variant (case#42 and 43).

Notably, three LS patients (case#5, 6 and 13) harbored cancers with *MLH1* promoter hypermethylation (Table 13 and Figure 17). Case#6 was particularly interesting and it was recently published by Cini et al. [44]: the MLPA germline analysis of this case (confirmed with long-range PCR and direct sequencing) identified a 997 nucleotide deletion in *MLH1* promoter and exon 1 sequences (MLH1 c.-68_c.116+713). This germline alteration was associated to a constitutional *MLH1* promoter hypermethylation (secondary epimutation) and bisulfite sequencing confirmed that the deletion and *MLH1* promoter methylation were observed *in cis*.

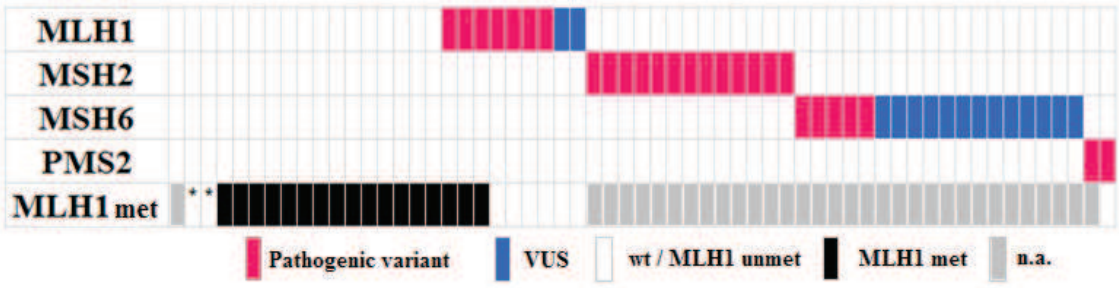

Figure 17. Germline MMR mutational landscape and MLH1 promoter methylation status of 59 MMR defective GCs (59 IHC MMR defective cases and 1 IHC MMR proficient and MSI case). Top panels represent the presence (pink, pathogenic variant or blue, variant with uncertain significance) or the absence (white) of MMR germline variants. The bottom panel indicates samples with *MLH1* promoter methylation (black) or without *MLH1* promoter methylation (white).

n.a.=not analyzed samples (gray); * IHC MLH1-PMS2 negative, no MMR germline variants identified, *MLH1* unmethylated (case#42 and 43)

3. NGS ANALYSIS ON ENDOMETRIAL CANCER

3.1 Targeted gene sequencing on 35 endometrial cancers

Targeted exome sequencing analysis of 16 genes involved in endometrial carcinogenesis through genetic and epigenetic mechanisms, was carried out on 35 endometrial cancers (ECs) of our cohort, for which sufficient and good quality DNA was available. As shown in Supplementary Table 1, this set of ECs was composed of 18 LS-related cancers (12 with MMR pathogenic variants and six with MMR VUS), two MMR deficient cancers of patients without any MMR germline mutation but characterized by a strong family history suggestive of Lynch syndrome (familial ECs), five MSI sporadic cancers (*MLH1* promoter methylated ECs) and 10 MSS sporadic cancers (Figure 18).

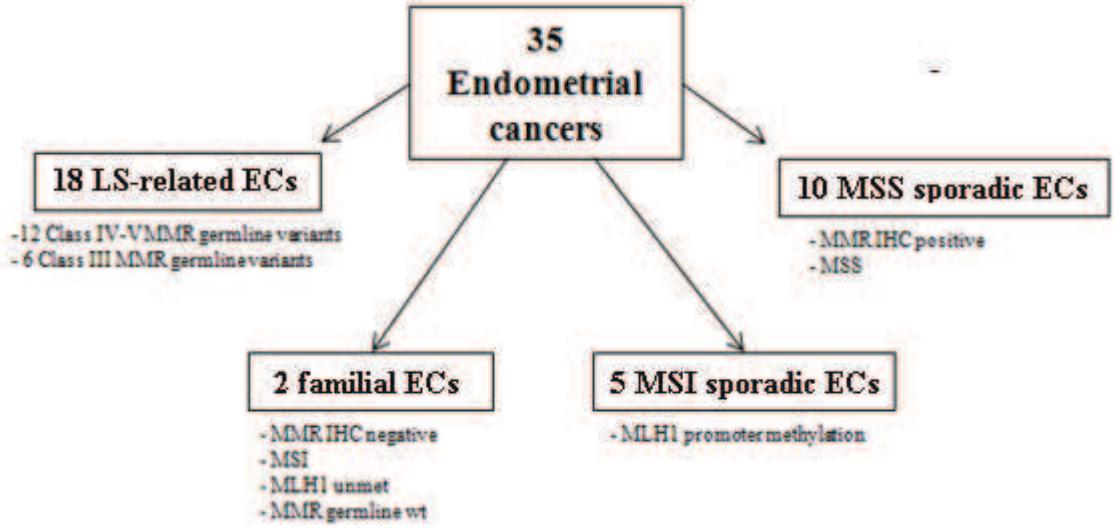

Figure 18. Endometrial cancers analyzed by targeted gene sequencing.

Data were filtered with a coverage of at least 200X and a mutated allelic fraction of at least 5%, according to NGS recommendations on FFPE samples [84]. Although we observed a variable coverage among samples, the number of reads for each analysis was often higher than 200X, with a mean coverage of 857 reads (range from 200 to 9169 reads).

We identified 465 somatic variants mapping in exon regions, UTR or canonical splicing sites, which were considered not to be polymorphisms. As shown in Figure 19, these mutations were represented by 266 missense variants, 104 variants in non coding regions (66 variants in splice donor or acceptor sites, 38 variants in UTR regions), 50 frameshift variants, 27 stop codon variants and 18 in frame insertion/deletions. It is interesting to note

that while most genes showed a high frequency of missense variants, *MSH2* and *ARID2* were mainly characterized by splice variants and *PTEN* and *ARID1A* exhibited a high number of frameshift mutations (Figure 19). Moreover, *POLE, ARID1A, ARID2*, *EZH2*, *SMARCA4* and *MSH2* were significantly more mutated than the other genes (50 vs 13 mean mutations respectively, p<0.0001, Figure 19).

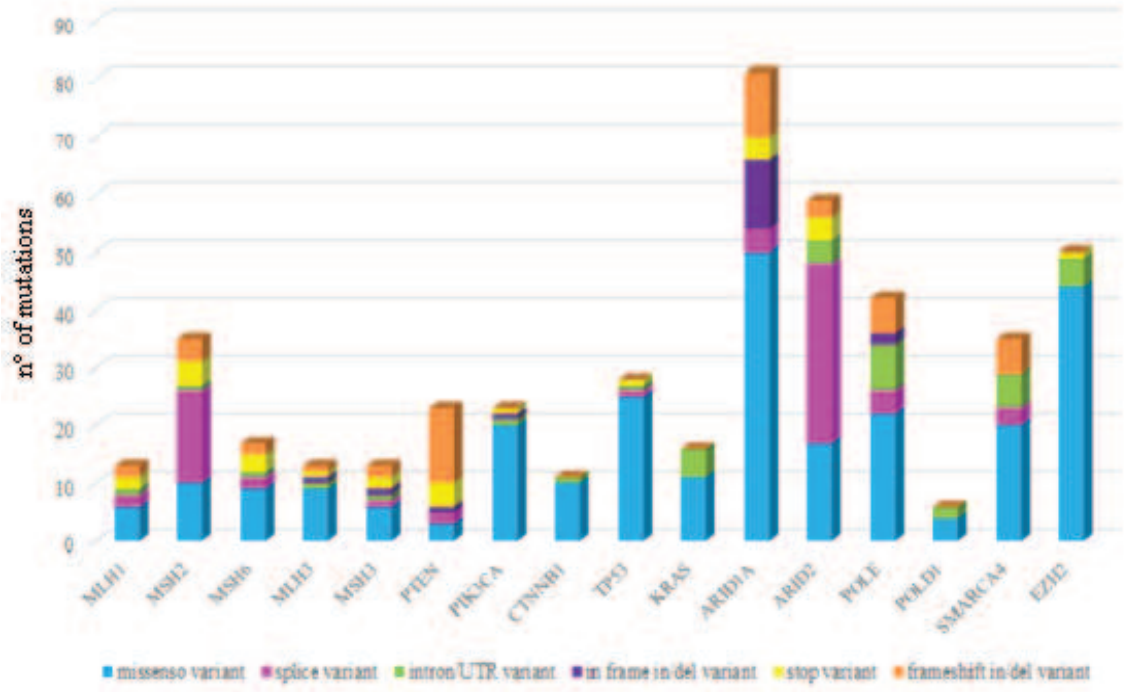

Figure 19. Distribution of somatic variants identified in each gene analyzed.

For each gene, we considered the average of mutated allele fractions (AF) in order to identify putative driver genes. This analysis highlighted that five genes, namely *MSH2*, *PTEN*, *CTNNB1*, *KRAS* and *ARID2,* showed significantly higher AF with respect to the remaining genes (22.6% vs 12.4%, p=0.0007, Figure 20). These findings allowed us to consider these five genes as driver gene in our cohort.

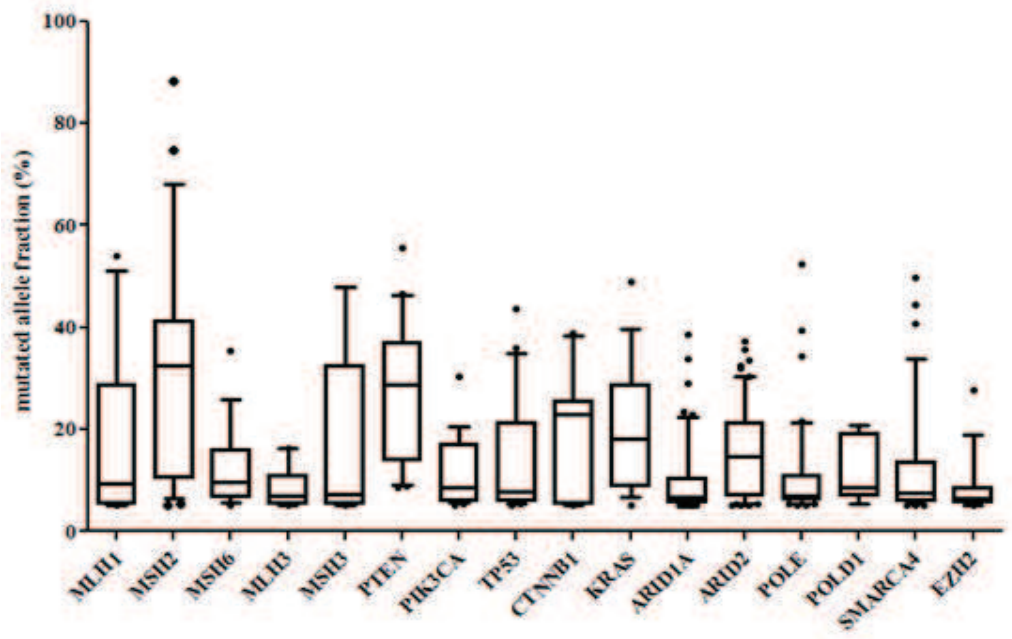

Figure 20. Distribution of mutated allele fractions observed for each gene analyzed. Mutated allele fraction is defined as the percentage of reads that carried the mutation versus the total reads.

Moreover, we found a significant correlation between the number of mutations and the microsatellite instability status as, the mean number of variants for each gene was significantly higher in MSI cases than MSS ECs (22 vs 4, $p<0.0001$, Figure 21).

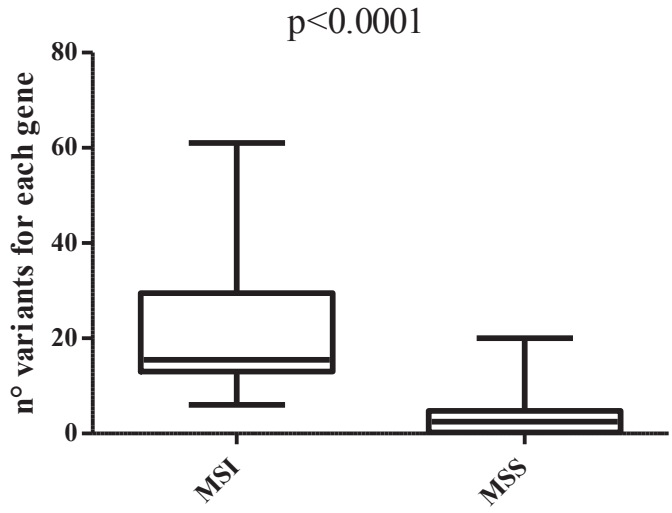

Figure 21. Distribution of the number of variants for each gene in MSI and MSS groups.

Furthermore, we detected recurrent gene variants in multiple cases as listed in Table 14. Interestingly, these mutations were only observed in *MSH2, TP53*, *KRAS*, *ARID1A*, *ARID2,*

POLE and *SMARCA4* genes. To verify the hypothesis that such mutations could have been the results of a defective MMR system, we investigated whether these variants preferentially occurred in repetitive or microsatellite sequences and if their distribution was prevalent in MSI cases. However, none of them fell in a repetitive sequence, except for a deletion of a trinucleotide in a context of eight repetitions (*ARID1A* c. 3999_4001delGCA); moreover, these variants were randomly present in both MSI and MSS cases.

Table 14. Detailed list of the more represented somatic variants.

Gene	Somatic variant	Type of variant	Impact*	LS ECs (18)	familial ECs (2)	MSI sporadic ECs (5)	MSS sporadic ECs (10)	Mean AF
MSH2	c.212-4delT	splice	MED	5	1	2	2	37.3%
	c.1881_1884delAGGA	frameshift	HIGH	4	0	0	0	73.5%
TP53	c.359A>G	missense	MED	3	0	3	4	9.5%
KRAS	c.35G>A	missense	MED	2	0	4	3	23.8%
	c.38G>A	missense	MED	1	0	0	1	26.7%
ARID1A	c. 3999_4001delGCA	in frame	MED	3	1	2	5	6.4%
	c.5945T>C	missense	MED	10	2	4	9	7.6%
ARID2	c.1023+2T>G	splice	HIGH	12	2	5	10	20.5%
POLE	c.4337_4338delTG	frameshift	HIGH	2	2	1	0	6.7%
SMARCA4	c.2062_2063insTCCT	frameshift	HIGH	3	0	1	2	7.4%

Legend:*according to MuTect2 and Verdict software; AF=mutated allele fraction (%)

3.2 Targeted gene sequencing on familial and sporadic ECs

The NGS analysis of normal samples confirmed the presence of all germline MMR variants except for the *PMS2* variant in case#23 (this gene was not included in the gene panel) and a large *MLH1* rearrangement, which is known not to be detected by NGS analysis (case#6). In all but three LS-ECs (cases#25, 29I and 40), a somatic mutation was identified as second hit in the same germline-mutated MMR gene (Figure 22A). Interestingly, we observed a high number of *MSH2* somatic variants (frameshift or splicing variants) in 14 out of 18 LS cancers regardless of the germline variant. In addition, the other most frequently mutated genes in LS associated cancers were *PTEN*, *PIK3CA*, *ARID1A*, *ARID2*, *POLE* and *SMARCA4*.

NGS analysis of normal DNA of case#42 and 44 confirmed the absence of germline MMR mutations in these patients, according to the previous analyses by Sanger sequencing and MLPA. These two familial cases showed a similar somatic mutational profile characterized by mutations of *MSH2*, *ARID1A*, *ARID2* and *POLE* genes (Figure 22B). Notably, they both displayed the same *POLE* c.4337_4338delTG (mean allelic fraction of 5.65%), *ARID1A*

c.5945T>C (mean allelic fraction of 10.76%) and *ARID2* c.1023+2T>G (mean allelic fraction of 23.78%) somatic variants (Figure 22B). On the contrary, only case#42 displayed *PTEN* (allelic fraction 38%) and *SMARCA4* (allelic fraction 5.4%) mutations while case#44 showed a variant in *CTNNB1* (allelic fraction 23.5%).

As shown in Figure 22B, we observed *ARID1A*, *ARID2* and *KRAS* mutations in all *MLH1* methylated sporadic ECs. Notably, *KRAS* mutations were significantly associated to *MLH1* methylated sporadic ECs with respect to the other cases (p=0.01). In detail, all *MLH1* methylated ECs (case#47, 48, 49, 53 and 56) were mutated in *KRAS* gene, while six out of 18 LS cancers and four out of 10 MSS sporadic cases were *KRAS* mutated. Moreover, three out of five *MLH1* methylated sporadic ECs showed *PTEN* mutations with high mutated allelic fraction (mean allelic fraction of 38%).

As shown in Figure 22B, *PTEN*, *ARID1A* and *ARID2* were mutated in sporadic MSS ECs. Nevertheless, this group did not display any peculiar gene mutation profile.

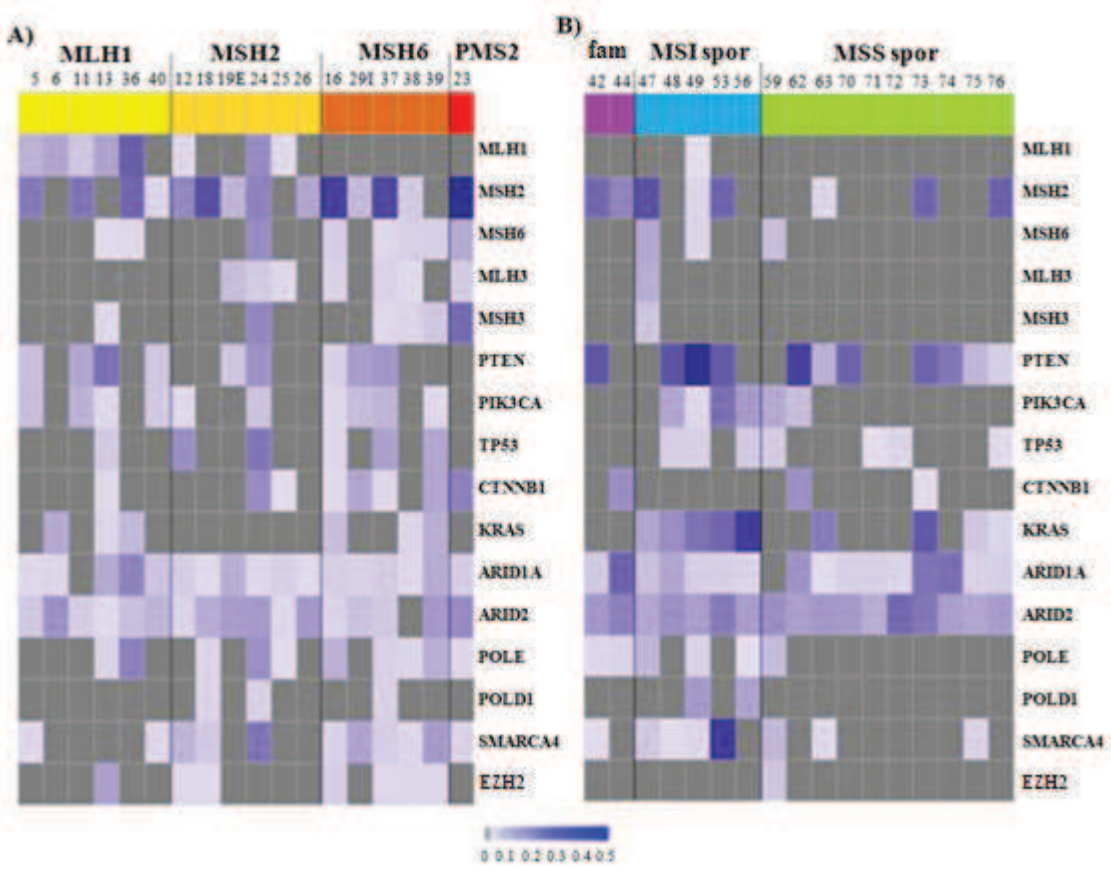

Figure 22. Heatmap showing the presence/absence of mutations for each gene (row) in Lynch Syndrome ECs (columns, in A) or familial/sporadic ECs (columns, in B). Mutations are reported for each patient in a blue color scale indicative of allelic fraction (from FA=5% in white to FA=50% in blue). Gray boxes indicate wild type sequences at a coverage of 200X. In panel A, top row reports the germline-mutated MMR genes. In panel B, familial ECs, sporadic MSI ECs (*MLH1* methylated ECs) and sporadic MSS ECs are reported.

3.3 Correlation of ARID1A mutations with IHC ARID1A expression

Based on the results obtained from targeted exome sequencing, we decided to investigate ARID1A protein expression using IHC analysis (Supplementary Table 1). An example of loss of expression of ARID1A protein is reported in Figure 23B.

Firstly, we preformed ARD1A IHC analysis on 33 out of 35 ECs analyzed with MiSeq (two cases were not available for the IHC analysis) and, secondly, we extended the analysis to our entire cohort (only 74 out of 80 GC cases were available). We regrouped the two familial cancers which belonged to patients with a strong family history suggestive for LS (case#42, 43 and 44) with LS related cases, calling them comprehensively familial cases.

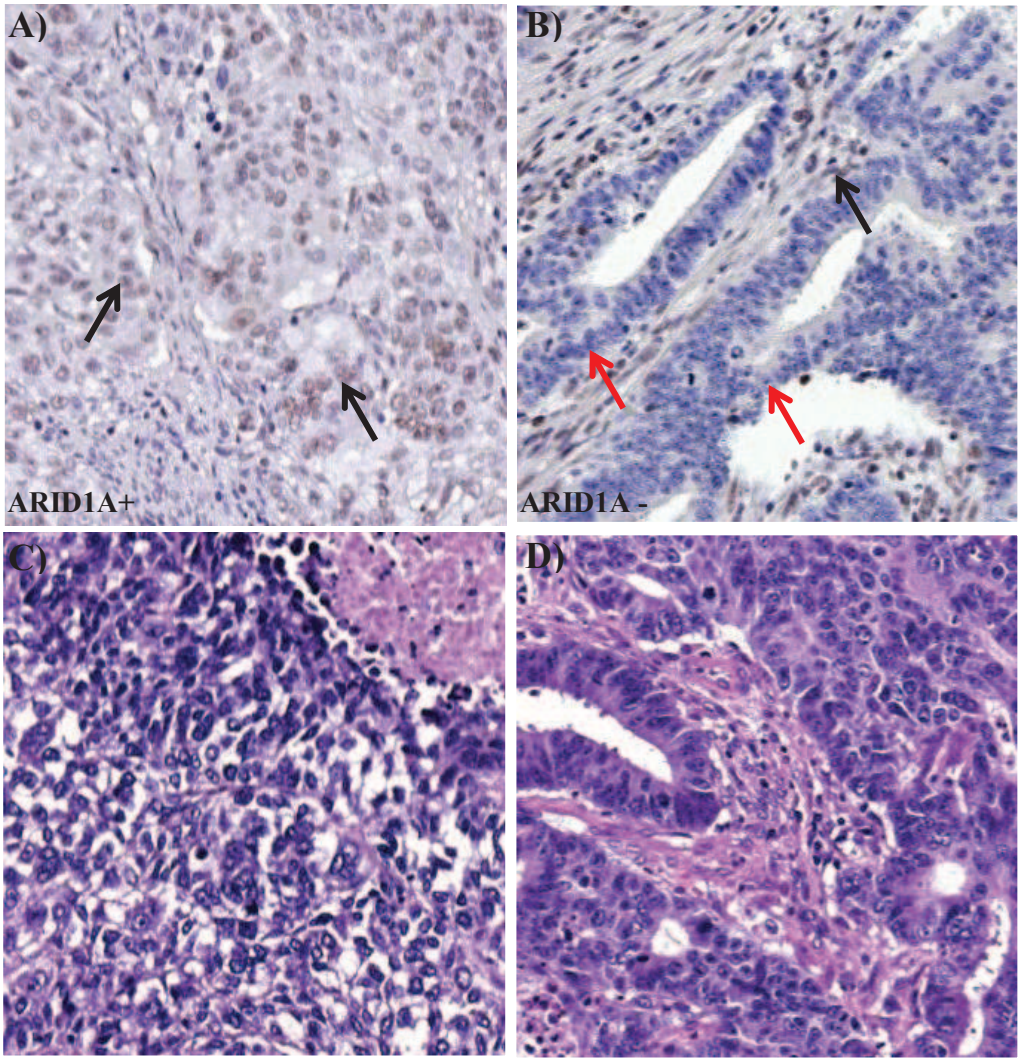

Figure 23. Examples of two endometrial cancers with positive IHC expression (A, black arrows) and loss of IHC expression of ARID1A protein (B, red arrows; positive nuclei of internal control cells, black arrow). Hematoxylin-eosin staining of the two representative cases (C and D, respectively).

IHC analysis identified nine cases showing ARID1A protein loss, five cases with a focal loss of the protein, while the remaining 19 cases did not show any protein loss. When we correlated these results with the presence of *ARID1A* mutations using a mutated allelic fraction higher than 5%, we did not observe any correlation. This result was not surprising since we detected at least one mutation in *ARID1A* gene in 31 out of 33 ECs with a mean AF of 10.4%. When we decided to consider only *ARID1A* mutations with a mutated allelic fraction higher than 10%, the concordance with IHC ARID1A test raised to 67.7% (21/31 cases, p=0.05). Moreover, when we extended the ARID1A IHC analysis to all our series (Figure 24), ARID1A loss of expression was significantly associated to familial cases (55%, 22/40 GCs) compared to MSI *MLH1* methylated GCs (23.1%, 3/13 GCs) or MSS sporadic cases (19%, 4/21 GCs, p=0.01).

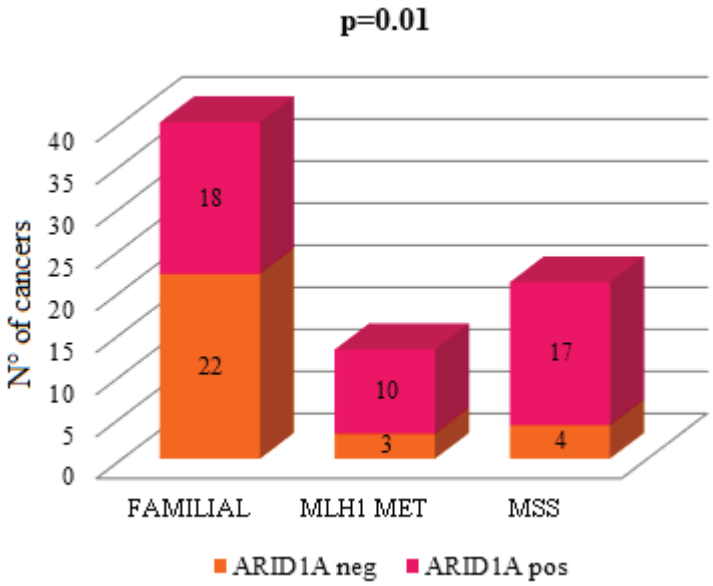

Figure 24. Distribution of ARID1A IHC results among the three groups (familial, MSI *MLH1* methylated sporadic and MSS sporadic GCs).

DISCUSSION

MMR-deficiency analysis is an efficient strategy to identify inherited and sporadic cancers characterized by microsatellite instability. The identification of MSI GCs is important because of the high incidence of MSI tumors among sporadic GCs (30%) [23], the earlier onset of these tumors with respect to colon cancers in LS female patients [36, 52], a favorable clinical outcome [60] and the potential relationship between MSI and efficacy of immune checkpoint inhibition [61].

We decided to select a cohort of patients who referred to Genetic Counseling Service in order to enrich the number of MMR deficient GCs. Indeed, IHC and MRP analysis identified a larger number of MMR deficient cases (59 GCs, 74%) than that reported in a consecutive series of GCs. Considering the immunophenotypical distribution of MMR IHC negative cases, we observed 25 MLH1/PMS2 negative cases (43%), 24 MSH2/MSH6 negative GCs (41%), eight MSH6-only negative tumors (14%) and one PMS2-only negative case (2%) in agreement with recent literature [88, 89].

Firstly, we observed a high concordance between MMR IHC analysis and MRP-MSI test (91.3%), confirming that both these two methods have a high sensitivity in the identification of MMR deficient cases in routine diagnostics. According to recent literature, most of discordant cases that we identified were characterized by the loss of a MMR protein expression and MSS phenotype (6 GCs). By contrast, we observed only one case showing MSI in absence of MMR protein expression alterations [64]. In spite of this increased sensitivity of IHC analysis, it must be considered that the IHC test requires a great experience in the technical set-up, as several critical issues may occur, including a correct staining assessment, a careful evaluation of internal normal controls, a cautious estimation of cases with focal expression of the proteins and the recognition of staining artifacts caused by technical problems [63].

On the other hand, different hypothesis have been proposed to explain the lower sensitivity of MSI test with respect to IHC analysis. Firstly, some authors have suggested that the current MSI panel does not include endometrial specific loci as it has been developed for the MSI study of colorectal and gastric sites [65]. Secondly, a recent NGS study aimed at identifying microsatellite instability in several human cancers revealed that the ECs showed the smallest difference between MSI and MSS groups for all instability metrics measured, suggesting that the inherent difficulty of the MSI test is caused more likely by a biological characteristic of GCs rather than the use of an unsuitable MSI panel [66].

Accordingly with this last hypothesis, in our work we identified a subset of ambiguous cases that did not fully meet MSI criteria (B-MSI) which were characterized by the presence of small microsatellite alterations (<3bp). It is interesting to note that B-MSI are frequently found among ovarian cases and they showed preferentially MSH2 and/or MSH6 negativity, in line with those reports describing an absent or mild MSI phenotype when MSH6 gene is involved [90-92].

The panel of additional tissue-specific loci that we tested resulted less useful with respect to MRP panel. In fact, we never observed alterations in *SVIL*, *JAK1*, *JMJD1C* and in two loci of *MBD6* gene while the remaining four loci (*RPL22*, *SRPR*, *MBD6_3* and *NRIP*) had a lower concordance with IHC with respect to MRP analysis (61% vs 91.3%, $p<0.0001$). However, we found an association between *RPL22* and MLH1 defects suggesting for the first time an involvement of *RPL22* as a target gene in the MLH1-driven pathogenesis. Furthermore, *RPL22* and *SRPR* should be studied in a larger cohort to evaluate their utility in supporting MRP panel for MSI testing as the frameshift deletion in *RPL22* locus was mostly exclusively found in MSI endometrial cancers even by the Cancer Genome Atlas Network [6].

Overall, these data suggest that the integrated use of IHC and microsatellite instability test is mandatory for a robust and sensitive MMR-deficiency analysis [64]. Together, these approaches compensate for each other's weaknesses and provide reliable data for the clinician and the geneticist.

The second aim of my PhD thesis regarded the characterization of the MMR deficiency in sporadic and hereditary GCs, identifying both germline MMR variants associated with Lynch syndrome and sporadic MSI cases associated with *MLH1* promoter methylation. The genetic counseling of all 76 patients together with MMR-deficiency results on GCs identified a subgroup of 56 patients (73.7%) who deserved MMR germline test. Moreover, the IHC analysis defined which MMR gene should be investigated first with germline test, as already observed in literature [36].

The analysis of MMR germline variants permitted to identify 18 Lynch syndrome patients carrier of a pathogenic mutation (IARC class IV-V variants, 46.4%) and allowed these patients and their relatives to participate to a specific program of prevention and surveillance. Moreover, we identified a variant with uncertain significance (VUS, IARC class III) in 14 out of 56 patients tested (25%) according to literature [93]. VUS represent those variants for which pathogenicity has not been demonstrated or excluded in published

literature and mutation databases (https://www.insight-group.org/). In our cohort, we observed a segregation of the MMR germline VUS with the disease in all analyzed families and according to this and to the family history we considered these patients as Lynch syndrome cases. Globally, we observed a higher percentage of *MSH6* germline variants (42%) with respect to other MMR mutations (*MSH2* 30%, *MLH1* 23% and *PMS2* 5%), in line with those papers that identify a higher number of *MSH6* germline variants in LS patients who display gynecological cancers [94]. Furthermore, sixteen out of 56 patients (28.6%) did not carry any MMR germline variant. All MMR wild-type patients except one (case#44) displayed a GCs characterized by the loss of IHC expression of MLH1/PMS2 proteins.

The *MLH1* methylation analysis was performed on all MLH1 IHC negative GCs (15 GCs belonging to MMR wild-type patients and 10 LS-related GCs) with MS-MLPA and bisulfite-pyrosequencing analysis. The MS-MLPA is the technique more widely used for *MLH1* promoter methylation definition because it detects all *MLH1* promoter regions [95]. On the other hand, the bisulfite-pyrosequencing analysis of *MLH1* promoter region C provides a quantitative evaluation of the methylation level [96] and, in our series, it was sufficient to identify all *MLH1* methylated samples. Interestingly, the MMR germline analysis together with *MLH1* promoter methylation test revealed three cases with both a germline pathogenic variant of *MLH1* and *MLH1* promoter methylation (Case#5, 6 and 13), suggesting a second hit of inactivation through *MLH1* epigenetic silencing. Differently, case#6 showed a rare secondary epimutation as described in Cini et al. characterized by a high somatic *MLH1* methylation level (more than 50%) and germline *MLH1* promoter methylation [27, 42, 44].

Finally, we identified three interesting cases (case#42, 43 and 44) belonging to three patients with a strong family history suggestive for LS: case#42 and 43 showed MLH1-PMS2 IHC loss and the absence of *MLH1* methylation and MMR germline variants; case#44 were MSH2-MSH6 IHC negative but no *MSH2* or *MSH6* germline mutations were identified. According to literature, 32% of patients with MMR deficiency display Lynch-like syndrome (LLS), which means that they are positive for the clinical criteria of LS (Bethesda revised and Amsterdam criteria) but they do not carry any MMR germline variant [97]. The cause of tumor MMR deficiency in Lynch-like syndrome cases is likely due to either unidentified germline MMR gene mutations, somatic cell mosaicism, or biallelic somatic inactivation [98].

The last aspect of my thesis concerned the characterization of the mutational profile of hereditary and sporadic endometrial cancers using a targeted exome sequencing panel of 16 genes involved in endometrial carcinogenesis through genetic and epigenetic mechanisms [6, 78-82]. For the first time, we performed a targeted gene sequencing analysis on LS and LLS related cancers in comparison to sporadic ECs (with *MLH1* promoter methylation or MSS tumors), while the literature is focused on the mutational landscape of sporadic ECs characterized by different clinical or histopathological profiles [6, 35, 99-101].

Targeted exome sequencing was possible in the 35 ECs and matched normal tissues that in our cohort yielded sufficient and good quality DNA samples for NGS analysis. We decided to filter the data with a coverage of at least 200X and a mutated allele fraction of at least 5%, in line with recent recommendations using FFPE samples [84-87]. Although the range of minimum acceptable coverage varies between different studies, most researchers agree that in clinical samples the coverage should be more than 100X and that the variability in the total number of reads is an important parameter in order to exclude poor quality DNA samples. In this study, we carefully evaluated these technical aspects and we decided to adopt strict criteria during data analysis to confidently perform variant quantification [83].

The series examined by NGS analysis included almost exclusively endometrioid tumors (there was only one undifferentiated EC), encompassing a total of 25 MSI ECs and 10 MSS ECs. Firstly, we did a comparison between our results and NGS data reported by the Cancer Genome Atlas Network, currently the most comprehensive genomic, transcriptomic and proteomic characterization ever reported on ECs [6]. In this study the authors stratified endometrioid ECs into three main distinct molecular subgroups: 1) an ultra-mutated/*POLE* mutant group with a unique nucleotide change spectrum, 2) a hypermutated/MSI tumors group, mostly characterized by *MLH1* promoter methylation, 3) a group including most of the MSS endometrioid ECs, characterized by low mutation frequency and by low somatic copy number alterations. In agreement with this molecular classification, our study demonstrated that MSI ECs, including both LS/LLS and sporadic ones, showed a significantly higher mutational load than MSS ECs, with a mean of 22 somatic mutations per tumor in d-MMR group compared with four mutations per tumor in p-MMR subset. As already reported for MSI colorectal cancers, this result confirms that also MSI ECs, regardless of the origin (hereditary or sporadic) or type of mutation, are

hypermutated tumors and may be considered good candidates for checkpoint immunotherapy as recently shown in small clinical trials (https://clinicaltrials.gov/).

The Cancer Genome Atlas Network identified another possible ultramutated phenotype in ECs, that is characterized by somatic *POLE* mutations and, specifically by the two mutational hotspot p.V411L and p.P286R [6]. In our series, we did not find any case with this molecular profile, although we observed a high number of somatic *POLE* mutations mapping along the whole gene. These mutations were almost exclusively observed in MSI tumors (regardless of the hereditary or sporadic origin) and they were always low allelic fraction variants (mean allelic fraction of 11.1%) not reported in COSMIC database (cancer.sanger.ac.uk/). Although these variants did not occur in microsatellite within the coding sequences, altogether these observations suggest that *POLE* may be a target gene in MSI ECs and that "passenger" mutations at low allele frequency may contribute to exacerbate the mutator phenotype in these tumors [102].

An important finding of our study regards the comparison of LS/LLS ECs with sporadic MSI ECs. The NGS analysis of normal DNA of LS patients confirmed the presence of all the germline mutations previously identified in *MLH1*, *MSH2* or *MSH6* genes. The only exception was for a large *MLH1* rearrangement that could not be found by the target exon sequencing performed in this study.

In all but three LS-ECs a somatic mutation was identified as "second hit" in the same MMR gene with the germline mutation, suggesting that the somatic inactivation of the second allele frequently occurs by a mutational event in these cases. Interestingly, in addition to the biallelic inactivation of a specific MMR gene, a high frequency of *MSH2* somatic variants (frameshift or splicing variants) was observed in LS/LLS cancers regardless of the germline variant. Interestingly, these *MSH2* mutations showed high AF (Figure 20), suggesting a clonal selection of these mutations in the majority of LS/LLS ECs although, based on MSH2 immunohistochemical data, MSH2 protein expression was not compromised.

As expected, MSI sporadic ECs were characterized by *MLH1* methylation. Interestingly, although these cases showed complete loss of MLH1 protein, we never observed a biallelic methylation of the promoter. On the other hand, somatic mutations in MMR genes were less frequent in MSI sporadic ECs compared with LS/LLS ECs, and a *MLH1* mutation was observed in only one case (allelic fraction of 5.1%).

The main observation in MSI sporadic ECs was that *KRAS* mutations were significantly associated to *MLH1* methylation (p=0.01). In this work for the first time, we observed this correlation in ECs and appears to be very intriguing as recent literature demonstrated that specific pathways mediate *MLH1* silencing in *BRAF* or *KRAS* mutant colorectal cancers [103-105], suggesting a general model by which different oncoproteins can orchestrate promoter hypermethylation and transcriptional silencing of tumor-suppressor genes during cancer development.

Finally, considering the whole series of ECs examined by NGS, the most frequent mutated genes were *PTEN*, *ARID1A* and *ARID2*, regardless of MSI status (Figure 22). While *PTEN* is a well-known driver gene in endometrial endometrioid carcinogenesis, little is known about the involvement of *ARID* family genes, coding for proteins of SWI/SNF chromatin remodeling complex [106]. Indeed, recent informations on *ARID* genes are emerged from comprehensive genome-wide analyses by NGS. *ARID1A* mutations have been found in various types of cancer and occur at high frequency in endometrioid ECs and in endometriosis-associated ovarian cancer [107]. *ARID1A* mutations induces changes in expression of multiple genes, including *MLH1*, via chromatin remodeling dysfunction and have been shown to be associated to PI3K-AKT alterations in many immunohistochemical works [30, 107-109]. Moreover, in a recent WES analysis of 13 ECs conducted by Liang and colleagues, they identified 12 potential driver genes for endometrial carcinogenesis including *ARID1A* and demonstrated the role of this gene as a novel regulator of PI3K pathway activity [90]. Since *ARID1A* mutations occur at the early stage of ECs, availability of a screening method for the detection of *ARID1A* mutations together with the activation of PI3K/AKT pathway would be very useful for early diagnosis of ECs. To this regard, the immunohistochemical analysis of ARID1A has been proposed as a quick and economic surrogate of mutation analysis, as it was suggested that mutations spanning the whole gene are highly correlated with loss of protein expression [30]. In this study, we evaluated the immunohistochemical expression of ARID1A in 74 GCs of our cohort, composed by 58 endometrial cancers (ECs), 12 ovarian carcinomas and four endocervical cancers. We found loss of expression of ARID1A protein in 39% of the tumors, in agreement with the recent literature [107]. Moreover, we performed a preliminary correlation between loss of IHC expression of ARID1A and the mutation status of the gene in the subset of the 33 ECs examined by NGS. For this analysis we decided to only include *ARID1A* mutations with a mutated

allelic fraction higher than 10% (excluding low allelic fraction variants ranging from 5% to 10%) and we obtained a concordance of 67.7% that globally reflects data previously reported [107].

A novel finding in this study was the observation that ARID1A IHC loss is significantly associated to LS/LLS related cancers compared to sporadic GCs (p=0.01). Although these data should be validated in a larger cohort, they suggest a different involvement of SWI/SNF complex in the familial endometrial carcinogenesis with respect to the sporadic one.

This study presented some limitations. First, we could not provide correlations with prognosis as a complete and long-term follow-up was not available for all patients. Secondly, the analyses were conducted on a small size cohort, as we decided to include only suspected LS patients in our series. Finally, as the NGS results were collected at the end of the PhD internee, we could not validate these findings with a second approach such as Sanger sequencing or qPCR. Nevertheless, we plan to develop a prospective research work starting from the thesis results, in order to improve these limitations.

In conclusion, the combined use of MMR IHC analysis and MRP-MSI test is a sensitive and reliable strategy to identify MMR deficient GCs. The analysis of coding microsatellites in *RPL22* and *SRPR* genes as well as *MLH1* promoter methylation test can be useful in the evaluation of ambiguous MSI GCs.

A comparative analysis of genetic and epigenetic features of LS/LLS and sporadic ECs provides useful insights into disease biology and diagnostic classification of these tumors. Integrated analysis of germline mutations in MMR genes, *MLH1* promoter methylation and somatic mutations in a small panel of driver genes for ECs allows the recognition of peculiar molecular subgroups that may impact on clinical management of these patients. Figure 25 reports a schematic presentation of the relevant points of this work.

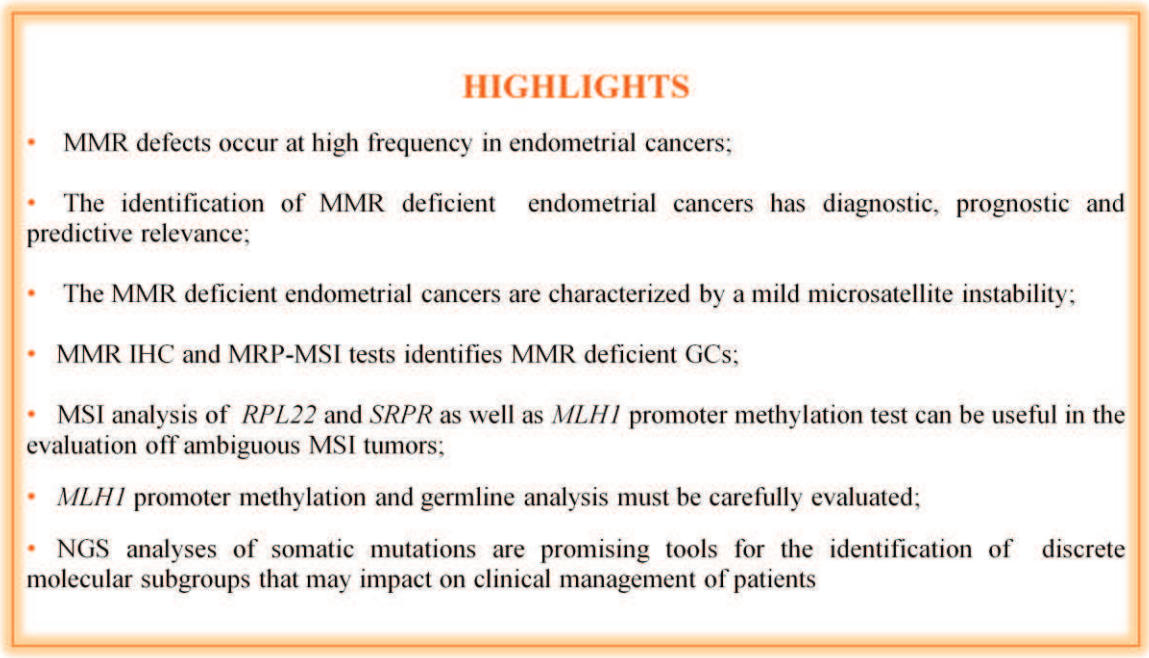

Figure 25. Schematic presentation of the relevant points.

SUPPLEMENTARY TABLE

Supplementary Table 1. Comprehensive data of 80 gynecological cancers

P ID	T ID	Site	Histotype	G	IHC	MRP MSI							Additional loci analysis				Germline mutation		MLH1 met	IHC ARID1A
						MSI	NR21	BAT26	BAT25	NR24	NR22	Shape	RPL22	SRPR	MBD6_3	NRIP1	Germline variant	IARC class		
2	2	Ov	Serous	3	MLH1-PMS2 neg	MSI	-5	-8	-3	-3	-3	+	MUT	wt	wt	wt	MLH1 del ex8	5	U	-
3	3	End	Endom	1		MSI	-2	-4	-4	-1	-4	+	MUT	wt	wt	wt	MLH1 c.1459C>T	5	U	+
4	4	Cerv	Endom	2		MSI	-4	-8	-6	-3	-3	+	MUT	wt	wt	wt	MLH1 c.1459C>T	5	U	-
5	5*	End	Endom	1		MSI	-1	-3	-5	-3	-2	+	MUT	wt	wt	MUT	MLH1 c.1852delAAG	5	M	-
6	6*	End	Endom	1		MSI	-7	-11	-7	-7	-5	+	MUT	MUT	wt	wt	MLH1 c.-68_c.116+713	5	M	+
13	13*	End	Endom	1		MSI	-1	-3	-1	-3	s	+	MUT	wt	wt	wt	MLH1 c.458_462delAGGAC	5	M	+
23	23*	End	Endom	2		MSI	-5	-4	1	-2	s	+	wt	wt	wt	wt	PMS2 c.137G>T	5	U	+
36	36*	End	Endom	2		MSI	-4	-6	-7	-3	-5	+	wt	MUT	MUT	wt	MLH1 c.440G>A	3	U	+
42	42*	End	Endom	2		MSI	-2	-1	-3	-3	-2	+	wt	wt	wt	wt	wt		U	-
46	46 E	End	Endom	1		MSI	-3	-4	-5	-3	-3	+	wt	wt	wt	wt	wt		M	-
	46 O	Ov	Mucinous	1		MSI	-3	-3	-4	-1	-2	+	MUT	wt	wt	wt			M	+
47	47*	End	Endom	1		MSI	-1	-2	-4	-3	-1	+	wt	MUT	wt	wt	wt		M	+
48	48*	End	Endom	2		MSI	-2	-4	-1	-3	-1	+	wt	wt	wt	wt	wt		M	na
49	49*	End	Endom	3		MSI	-1	-3	-4	-6	-1	+	MUT	wt	wt	wt	wt		M	-
50	50	End	Endom	3		MSI	-2	-3	-3	-3	s	+	MUT	wt	wt	MUT	wt		M	+
51	51	End	Clear Cell	3		MSI	-1	-3	-7	-4	-2	+	ne	ne	ne	ne	wt		M	+
52	52	End	Clear Cell	3		MSI	-2	-4	-2	-3	-3	+	MUT	wt	wt	wt	wt		M	+
53	53*	End	Endom	1		MSI	-5	-3	-3	-2	-3	+	MUT	wt	wt	wt	wt		M	+
56	56*	End	Endom	2		MSI	-2	-5	-4	-3	s	+	MUT	wt	wt	wt	wt		M	+
11	11*	End	Endom	1		B-MSI	-1	-1	-1	-4	-1	+	wt	wt	wt	wt	MLH1 c.790+1G>A	3	U	+
41	41	End	Endom	1		B-MSI	-2	-2	-4	-2	-1	+	wt	wt	wt	wt	wt		M	+
43	43	End	Endom	2		MSS	s	-1	s	s	s	-	wt	wt	wt	wt	wt		U	+
45	45	Ov	Mixed	2		MSS	s	s	s	s	s	-	wt	wt	wt	wt	wt		M	+

54	54	End	Endom	2		MSS	s	-1	-3	s	s	-	ne	ne	ne	ne	wt		M	+
55	55	End	Endom	2		MSS	-1	s	s	s	s	-	MUT	wt	wt	wt	wt		M	-
22	22	End	Undif	3	PMS2 neg	MSI	-4	-5	-5	-4	-1	+	wt	wt	wt	wt	PMS2 c.2123delA	5		-
1	1	End	Endom	2	MSH2-MSH6 neg	MSI	-3	-4	-8	-5	-3	+	wt	wt	ne	wt	MSH2 del ex1-6	5		-
7	7	End	Endom	1		MSI	-4	-9	-6	-5	-3	+	wt	MUT	wt	wt	MSH2 ivs5(+3)A>T	5		-
8	8	End	Endom	1		MSI	-4	-4	-2	-7	-3	+	wt	wt	wt	wt	MSH2 del ex1-6	5		-
12	12*	End	Endom	2		MSI	-4	-6	-3	-7	-1	+	wt	wt	wt	wt	MSH2 c.942+3A>T	5		+
15	15	End	Endom	1		MSI	-1	-6	-1	-1	-3	+	wt	wt	wt	wt	MSH2 del ex3-6	5		na
16	16*	End	Endom	2		MSI	-5	-7	-4	-5	-1	+	wt	wt	wt	wt	MSH6 c.2764C>T	5		+
18	18*	End	Mixed	3		MSI	s	-3	3	-1	-3	+	wt	wt	wt	wt	MSH2 c.839T>A	5		-
19	19 C	Cerv	Endom	2		MSI	-1	-6	-4	-2	-2	+	wt	wt	wt	wt	MSH2 c.839T>A	5		-
	19 E*	End	Endom	3		MSI	-2	-3	3	-5	-2	+	MUT	MUT	wt	wt				-
24	24*	End	Endom	3		MSI	s	-3	s	-3	-2	+	wt	wt	wt	wt	MSH2 c.892C>T	5		-
25	25*	End	Endom	2		MSI	-1	-4	-4	-2	-2	+	wt	wt	wt	wt	MSH2 c.715C>T	5		na
26	26*	End	Endom	1		MSI	-6	-5	-2	-3	-3	+	MUT	wt	wt	wt	MSH2 c.34dupG	5		+
27	27	Isth	Endom	2		MSI	-1	-3	-3	s	s	+	wt	wt	ne	wt	MSH6 c.*(23_26)dupAGTT	3		-
28	28	End	Mixed	2		MSI	s	-4	-4	-2	s	+	wt	wt	wt	wt	MSH6 c.*(23_26)dupAGTT	3		na
29	29 O	Ov	Endom	2		MSI	-3	-3	-4	-1	-2	+	wt	wt	wt	wt	MSH6 c.*(23_26)dupAGTT	3		+
	29 I*	Isth	Endom	3		MSI	-1	-4	-4	-3	-2	+	wt	wt	wt	wt				+
30	30	Ov	Endom	2		MSI	-2	-4	-6	-2	s	+	ne	ne	ne	ne	MSH6 c.*(23_26)dupAGTT	3		+
34	34	Isth	Endom	-		MSI	-3	-4	-4	-3	-2	+	wt	wt	wt	wt	MSH6 c.*(23_26)dupAGTT	3		+
35	35*	End	Mixed	3		MSI	-4	-10	-4	-4	s	+	MUT	wt	wt	wt	MSH6 c.642C>T	3		+
37	37*	End	Mixed	3		MSI	-4	-4	-3	-5	-2	+	wt	MUT	wt	wt	MSH6 c.*(23_26)dupAGTT	3		-
44	44*	End	Endom	3		MSI	-1	-4	-5	-2	-2	+	MUT	MUT	wt	wt	wt			-
9	9	Ov	Endom	2		B-MSI	-3	-1	-1	-1	-1	+	MUT	MUT	wt	wt	MSH2 c.1216C>T	5		-
10	10	Isth	Endom	2		B-	-2	s	-4	-2	-1	+	wt	MUT	wt	wt	MSH2 c.229-230delAG	5		-

33	33	Ov	Mixed	3		MSI B-MSI	1	1	-3	-2	1	+	MUT	wt	wt	wt	MSH6 c.*(23_26)dupAGTT	3		-
17	17	End	Endom	2	MSH6 neg	MSI	-5	-2	-1	-1	-3	+	wt	wt	wt	wt	MSH6 c.2764C>T	5		-
31	31	End	Endom	1		MSI	s	-4	-4	-2	s	+	MUT	wt	wt	wt	MSH6 c.3632T>C	3		-
14	14	End	Endom	1		B-MSI	s	-2	-2	-1	-1	+	wt	wt	wt	wt	MSH6 c.3261delC	5		+
20	20	Ov	Carcinosarcoma	3		B-MSI	-1	-1	-2	-1	s	+	wt	wt	wt	wt	MSH6 c.931_935delAAAA	5		-
21	21	End	Endom	-		B-MSI	-1	-2	-1	-2	-2	+	wt	wt	wt	wt	MSH6 c.4002-23_4002-10del	5		ne
32	32	Ov	Mixed	2		B-MSI	s	-1	1	-2	1	+	wt	wt	wt	wt	MSH6 c.3632T>C	3		ne
38	38*	End	Endom	1		MSS	s	s	s	s	s	-	wt	wt	wt	wt	MSH6 c.2314C>T	3		+
39	39*	End	Undif	3		MSS	s	-1	s	s	s	-	wt	wt	wt	wt	MSH6 c.1184G>A	3		+
40	40*	End	Endom	2	p-MMR	MSI	-3	s	-3	s	-1	+	MUT	wt	wt	wt	MLH1c.1896+17T>C	5	U	+
57	57	End	Endom	1		MSS	s	s	s	s	s	-	wt	wt	wt	wt				+
58	58	End	Endom	1		MSS	s	s	s	s	s	-	wt	wt	wt	wt				+
59	59 E*	End	Endom	1		MSS	s	s	s	s	s	-	wt	wt	wt	wt				+
	59 O	Ov	Endom	1		MSS	s	s	s	s	s	-	wt	wt	wt	wt				+
60	60	Ov	Endom	2		MSS	s	s	s	s	s	-	wt	wt	wt	wt				+
61	61	End	Endom	1		MSS	s	s	s	s	s	-	wt	wt	wt	wt				+
62	62*	End	Endom	2		MSS	s	s	s	s	s	-	wt	wt	wt	wt				-
63	63*	End	Endom	2		MSS	s	s	s	s	s	-	wt	wt	wt	wt				+
64	64	Cerv	Endom	1		MSS	s	s	s	s	s	-	wt	wt	wt	wt				+
65	65	End	Endom	2		MSS	s	s	s	s	s	-	wt	wt	wt	wt				+
66	66	Cerv	Serous	3		MSS	s	s	s	s	s	-	wt	wt	wt	wt				+
67	67	End	Endom	1		MSS	s	s	-3	s	s	-	wt	wt	wt	wt				-
68	68	Ov	Endom	3		MSS	s	s	-4	s	s	-	wt	wt	wt	wt				-
69	69	Ov	Endom	2		MSS	s	s	s	s	s	-	ne	wt	ne	wt				+

70	70*	End	Endom	2		MSS	s	s	s	s	s	-	wt	wt	wt	wt			+
71	71*	End	Endom	1		MSS	s	s	s	s	s	-	wt	wt	wt	wt			+
72	72*	End	Endom	2		MSS	s	s	s	s	s	-	wt	wt	wt	wt			+
73	73*	End	Mixed	3		MSS	s	s	s	s	s	-	wt	wt	wt	wt			-
74	74*	End	Endom	2		MSS	s	s	s	s	s	-	wt	wt	wt	wt			+
75	75*	End	Endom	1		MSS	s	s	s	s	s	-	wt	wt	wt	wt			+
76	76*	End	Endom	1		MSS	s	s	s	s	s	-	wt	wt	wt	wt			+

Legend: P ID= patient identification, T ID= tumor identification, *=cases analyzed with NGS; **SITE:** End=corpus of endometrium, Ov=ovary Cerv=endocervix, Isth=isthmus; **HISTOTYPE:** Endom=endometrioid, Undif=undifferentiated; **MMR IHC:** pro-MMR=proficient MMR system; **MRP test:** MSS=microsatellite stable, MSI=microsatellite unstable, B-MSI=microsatellite borderline; **Additional loci:** MUT=new locus unstable, wt=wild-type, ne=not evaluable; **germline analysis:** IARC=International Agency for Research on Cancer; **methylation analysis:** *MLH1* met=*MLH1* promoter methylation, M=methylated, U=unmethylated; **ARID1A IHC:** +positive, -negative, ne=not evaluable.

BIBLIOGRAPHY

[1] Ferlay J, Steliarova-Foucher E, Lortet-Tieulent J, Rosso S, Coebergh JW, Comber H, Forman D, Bray F. Cancer incidence and mortality patterns in Europe: estimates for 40 countries in 2012. Eur J Cancer 2012;49:1374-403.
[2] Bokhman JV. Two pathogenetic types of endometrial carcinoma. Gynecol Oncol 1983;15:10-7.
[3] Prat J, Gallardo A, Cuatrecasas M, Catasus L. Endometrial carcinoma: pathology and genetics. Pathology 2007;39:72-87.
[4] Chang YN, Zhang Y, Wang YJ, Wang LP, Duan H. Effect of hysteroscopy on the peritoneal dissemination of endometrial cancer cells: a meta-analysis. Fertil Steril 2011;96:957-61.
[5] Wiegand KC, Lee AF, Al-Agha OM, Chow C, Kalloger SE, Scott DW, Steidl C, Wiseman SM, Gascoyne RD, Gilks B, Huntsman DG. Loss of BAF250a (ARID1A) is frequent in high-grade endometrial carcinomas. J Pathol 2011;224:328-33.
[6] Kandoth C, Schultz N, Cherniack AD, Akbani R, Liu Y, Shen H, Robertson AG, Pashtan I, Shen R, Benz CC, Yau C, Laird PW, Ding L, Zhang W, Mills GB, Kucherlapati R, Mardis ER, Levine DA. Integrated genomic characterization of endometrial carcinoma. Nature 2013;497:67-73.
[7] Nicolae A, Preda O, Nogales FF. Endometrial metaplasias and reactive changes: a spectrum of altered differentiation. J Clin Pathol 2011;64:97-106.
[8] Cirisano FD, Jr., Robboy SJ, Dodge RK, Bentley RC, Krigman HR, Synan IS, Soper JT, Clarke-Pearson DL. The outcome of stage I-II clinically and surgically staged papillary serous and clear cell endometrial cancers when compared with endometrioid carcinoma. Gynecol Oncol 2000;77:55-65.
[9] Soslow RA, Bissonnette JP, Wilton A, Ferguson SE, Alektiar KM, Duska LR, Oliva E. Clinicopathologic analysis of 187 high-grade endometrial carcinomas of different histologic subtypes: similar outcomes belie distinctive biologic differences. Am J Surg Pathol 2007;31:979-87.
[10] Alkushi A, Kobel M, Kalloger SE, Gilks CB. High-grade endometrial carcinoma: serous and grade 3 endometrioid carcinomas have different immunophenotypes and outcomes. Int J Gynecol Pathol 2010;29:343-50.
[11] Tafe LJ, Garg K, Chew I, Tornos C, Soslow RA. Endometrial and ovarian carcinomas with undifferentiated components: clinically aggressive and frequently underrecognized neoplasms. Mod Pathol 2010;23:781-9.
[12] A.I.O.M. AIdOM. Neoplasie dell'utero: endometrio e cervice. 2015. Available at: http://www.aiom.it/professionisti/documenti-scientifici/linee-guida/utero-endometrio-cervice/1,784,1, Acessed.
[13] Fishel R. Mismatch repair, molecular switches, and signal transduction. Genes Dev 1998;12:2096-101.
[14] Grady WM, Carethers JM. Genomic and epigenetic instability in colorectal cancer pathogenesis. Gastroenterology 2008;135:1079-99.
[15] Palombo F, Iaccarino I, Nakajima E, Ikejima M, Shimada T, Jiricny J. hMutSbeta, a heterodimer of hMSH2 and hMSH3, binds to insertion/deletion loops in DNA. Curr Biol 1996;6:1181-4.
[16] Genschel J, Littman SJ, Drummond JT, Modrich P. Isolation of MutSbeta from human cells and comparison of the mismatch repair specificities of MutSbeta and MutSalpha. J Biol Chem 1998;273:19895-901.
[17] Littman SJ, Fang WH, Modrich P. Repair of large insertion/deletion heterologies in human nuclear extracts is directed by a 5' single-strand break and is independent of the mismatch repair system. J Biol Chem 1999;274:7474-81.
[18] McCulloch SD, Gu L, Li GM. Bi-directional processing of DNA loops by mismatch repair-dependent and -independent pathways in human cells. J Biol Chem 2003;278:3891-6.
[19] Lengauer C, Kinzler KW, Vogelstein B. Genetic instability in colorectal cancers. Nature 1997;386:623-7.
[20] Umar A, Buermeyer AB, Simon JA, Thomas DC, Clark AB, Liskay RM, Kunkel TA. Requirement for PCNA in DNA mismatch repair at a step preceding DNA resynthesis. Cell 1996;87:65-73.
[21] Zhang Y, Yuan F, Presnell SR, Tian K, Gao Y, Tomkinson AE, Gu L, Li GM. Reconstitution of 5'-directed human mismatch repair in a purified system. Cell 2005;122:693-705.
[22] Baptiste BA, Jacob KD, Eckert KA. Genetic evidence that both dNTP-stabilized and strand slippage mechanisms may dictate DNA polymerase errors within mononucleotide microsatellites. DNA Repair (Amst) 2015;29:91-100.
[23] Bruegl AS, Ring KL, Daniels M, Fellman BM, Urbauer DL, Broaddus RR. Clinical Challenges Associated with Universal Screening for Lynch Syndrome-Associated Endometrial Cancer. Cancer Prev Res (Phila) 2016.
[24] Katabuchi H, van Rees B, Lambers AR, Ronnett BM, Blazes MS, Leach FS, Cho KR, Hedrick L. Mutations in DNA mismatch repair genes are not responsible for microsatellite instability in most sporadic endometrial carcinomas. Cancer Res 1995;55:5556-60.

[25] Kobayashi K, Matsushima M, Koi S, Saito H, Sagae S, Kudo R, Nakamura Y. Mutational analysis of mismatch repair genes, hMLH1 and hMSH2, in sporadic endometrial carcinomas with microsatellite instability. Jpn J Cancer Res 1996;87:141-5.
[26] Lim PC, Tester D, Cliby W, Ziesmer SC, Roche PC, Hartmann L, Thibodeau SN, Podratz KC, Jenkins RB. Absence of mutations in DNA mismatch repair genes in sporadic endometrial tumors with microsatellite instability. Clin Cancer Res 1996;2:1907-11.
[27] Esteller M, Levine R, Baylin SB, Ellenson LH, Herman JG. MLH1 promoter hypermethylation is associated with the microsatellite instability phenotype in sporadic endometrial carcinomas. Oncogene 1998;17:2413-7.
[28] Capel E, Flejou JF, Hamelin R. Assessment of MLH1 promoter methylation in relation to gene expression requires specific analysis. Oncogene 2007;26:7596-600.
[29] Deng G, Chen A, Hong J, Chae HS, Kim YS. Methylation of CpG in a small region of the hMLH1 promoter invariably correlates with the absence of gene expression. Cancer Res 1999;59:2029-33.
[30] Bosse T, ter Haar NT, Seeber LM, v Diest PJ, Hes FJ, Vasen HF, Nout RA, Creutzberg CL, Morreau H, Smit VT. Loss of ARID1A expression and its relationship with PI3K-Akt pathway alterations, TP53 and microsatellite instability in endometrial cancer. Mod Pathol 2013;26:1525-35.
[31] Chunder N, Mandal S, Basu D, Roy A, Roychoudhury S, Panda CK. Deletion mapping of chromosome 1 in early onset and late onset breast tumors--a comparative study in eastern India. Pathol Res Pract 2003;199:313-21.
[32] Wilson BG, Roberts CW. SWI/SNF nucleosome remodellers and cancer. Nat Rev Cancer 2011;11:481-92.
[33] Wu JN, Roberts CW. ARID1A mutations in cancer: another epigenetic tumor suppressor? Cancer Discov 2013;3:35-43.
[34] Guan B, Wang TL, Shih Ie M. ARID1A, a factor that promotes formation of SWI/SNF-mediated chromatin remodeling, is a tumor suppressor in gynecologic cancers. Cancer Res 2011;71:6718-27.
[35] Liang H, Cheung LW, Li J, Ju Z, Yu S, Stemke-Hale K, Dogruluk T, Lu Y, Liu X, Gu C, Guo W, Scherer SE, Carter H, Westin SN, Dyer MD, Verhaak RG, Zhang F, Karchin R, Liu CG, Lu KH, Broaddus RR, Scott KL, Hennessy BT, Mills GB. Whole-exome sequencing combined with functional genomics reveals novel candidate driver cancer genes in endometrial cancer. Genome Res 2012;22:2120-9.
[36] Lynch HT, Lynch PM, Lanspa SJ, Snyder CL, Lynch JF, Boland CR. Review of the Lynch syndrome: history, molecular genetics, screening, differential diagnosis, and medicolegal ramifications. Clin Genet 2009;76:1-18.
[37] Martin-Lopez JV, Fishel R. The mechanism of mismatch repair and the functional analysis of mismatch repair defects in Lynch syndrome. Fam Cancer 2013;12:159-68.
[38] Thompson BA, Spurdle AB, Plazzer JP, Greenblatt MS, Akagi K, Al-Mulla F, Bapat B, Bernstein I, Capella G, den Dunnen JT, du Sart D, Fabre A, Farrell MP, Farrington SM, Frayling IM, Frebourg T, Goldgar DE, Heinen CD, Holinski-Feder E, Kohonen-Corish M, Robinson KL, Leung SY, Martins A, Moller P, Morak M, Nystrom M, Peltomaki P, Pineda M, Qi M, Ramesar R, Rasmussen LJ, Royer-Pokora B, Scott RJ, Sijmons R, Tavtigian SV, Tops CM, Weber T, Wijnen J, Woods MO, Macrae F, Genuardi M. Application of a 5-tiered scheme for standardized classification of 2,360 unique mismatch repair gene variants in the InSiGHT locus-specific database. Nat Genet 2014;46:107-15.
[39] Peltomaki P. Update on Lynch syndrome genomics. Fam Cancer 2016;15:385-93.
[40] Boland CR, Goel A. Microsatellite instability in colorectal cancer. Gastroenterology 2010;138:2073-87 e3.
[41] Knudson AG. Two genetic hits (more or less) to cancer. Nat Rev Cancer 2001;1:157-62.
[42] Peltomaki P. Epigenetic mechanisms in the pathogenesis of Lynch syndrome. Clin Genet 2014;85:403-12.
[43] Takeda T, Banno K, Yanokura M, Adachi M, Iijima M, Kunitomi H, Nakamura K, Iida M, Nogami Y, Umene K, Masuda K, Kobayashi Y, Yamagami W, Hirasawa A, Tominaga E, Susumu N, Aoki D. Methylation Analysis of DNA Mismatch Repair Genes Using DNA Derived from the Peripheral Blood of Patients with Endometrial Cancer: Epimutation in Endometrial Carcinogenesis. Genes (Basel) 2016;7.
[44] Cini G, Carnevali I, Quaia M, Chiaravalli AM, Sala P, Giacomini E, Maestro R, Tibiletti MG, Viel A. Concomitant mutation and epimutation of the MLH1 gene in a Lynch syndrome family. Carcinogenesis 2015;36:452-8.
[45] Hitchins MP, Wong JJ, Suthers G, Suter CM, Martin DI, Hawkins NJ, Ward RL. Inheritance of a cancer-associated MLH1 germ-line epimutation. N Engl J Med 2007;356:697-705.
[46] Goel A, Nguyen TP, Leung HC, Nagasaka T, Rhees J, Hotchkiss E, Arnold M, Banerji P, Koi M, Kwok CT, Packham D, Lipton L, Boland CR, Ward RL, Hitchins MP. De novo constitutional MLH1 epimutations confer early-

onset colorectal cancer in two new sporadic Lynch syndrome cases, with derivation of the epimutation on the paternal allele in one. Int J Cancer 2011;128:869-78.
[47] Suter CM, Martin DI, Ward RL. Germline epimutation of MLH1 in individuals with multiple cancers. Nat Genet 2004;36:497-501.
[48] Niessen RC, Hofstra RM, Westers H, Ligtenberg MJ, Kooi K, Jager PO, de Groote ML, Dijkhuizen T, Olderode-Berends MJ, Hollema H, Kleibeuker JH, Sijmons RH. Germline hypermethylation of MLH1 and EPCAM deletions are a frequent cause of Lynch syndrome. Genes Chromosomes Cancer 2009;48:737-44.
[49] Ward RL, Dobbins T, Lindor NM, Rapkins RW, Hitchins MP. Identification of constitutional MLH1 epimutations and promoter variants in colorectal cancer patients from the Colon Cancer Family Registry. Genet Med 2013;15:25-35.
[50] Morak M, Schackert HK, Rahner N, Betz B, Ebert M, Walldorf C, Royer-Pokora B, Schulmann K, von Knebel-Doeberitz M, Dietmaier W, Keller G, Kerker B, Leitner G, Holinski-Feder E. Further evidence for heritability of an epimutation in one of 12 cases with MLH1 promoter methylation in blood cells clinically displaying HNPCC. Eur J Hum Genet 2008;16:804-11.
[51] Barrow E, Hill J, Evans DG. Cancer risk in Lynch Syndrome. Fam Cancer 2013;12:229-40.
[52] Lu KH, Dinh M, Kohlmann W, Watson P, Green J, Syngal S, Bandipalliam P, Chen LM, Allen B, Conrad P, Terdiman J, Sun C, Daniels M, Burke T, Gershenson DM, Lynch H, Lynch P, Broaddus RR. Gynecologic cancer as a "sentinel cancer" for women with hereditary nonpolyposis colorectal cancer syndrome. Obstet Gynecol 2005;105:569-74.
[53] Vasen HF, Mecklin JP, Khan PM, Lynch HT. The International Collaborative Group on Hereditary Non-Polyposis Colorectal Cancer (ICG-HNPCC). Dis Colon Rectum 1991;34:424-5.
[54] Plaschke J, Kruger S, Dietmaier W, Gebert J, Sutter C, Mangold E, Pagenstecher C, Holinski-Feder E, Schulmann K, Moslein G, Ruschoff J, Engel C, Evans G, Schackert HK. Eight novel MSH6 germline mutations in patients with familial and nonfamilial colorectal cancer selected by loss of protein expression in tumor tissue. Hum Mutat 2004;23:285.
[55] Baglietto L, Lindor NM, Dowty JG, White DM, Wagner A, Gomez Garcia EB, Vriends AH, Cartwright NR, Barnetson RA, Farrington SM, Tenesa A, Hampel H, Buchanan D, Arnold S, Young J, Walsh MD, Jass J, Macrae F, Antill Y, Winship IM, Giles GG, Goldblatt J, Parry S, Suthers G, Leggett B, Butz M, Aronson M, Poynter JN, Baron JA, Le Marchand L, Haile R, Gallinger S, Hopper JL, Potter J, de la Chapelle A, Vasen HF, Dunlop MG, Thibodeau SN, Jenkins MA. Risks of Lynch syndrome cancers for MSH6 mutation carriers. J Natl Cancer Inst 2010;102:193-201.
[56] Jasperson KW, Tuohy TM, Neklason DW, Burt RW. Hereditary and familial colon cancer. Gastroenterology 2010;138:2044-58.
[57] Carcangiu ML, Radice P, Casalini P, Bertario L, Merola M, Sala P. Lynch syndrome--related endometrial carcinomas show a high frequency of nonendometrioid types and of high FIGO grade endometrioid types. Int J Surg Pathol 2010;18:21-6.
[58] Garg K, Shih K, Barakat R, Zhou Q, Iasonos A, Soslow RA. Endometrial carcinomas in women aged 40 years and younger: tumors associated with loss of DNA mismatch repair proteins comprise a distinct clinicopathologic subset. Am J Surg Pathol 2009;33:1869-77.
[59] Black D, Soslow RA, Levine DA, Tornos C, Chen SC, Hummer AJ, Bogomolniy F, Olvera N, Barakat RR, Boyd J. Clinicopathologic significance of defective DNA mismatch repair in endometrial carcinoma. J Clin Oncol 2006;24:1745-53.
[60] Kato M, Takano M, Miyamoto M, Sasaki N, Goto T, Tsuda H, Furuya K. DNA mismatch repair-related protein loss as a prognostic factor in endometrial cancers. J Gynecol Oncol 2015;26:40-5.
[61] Colle R, Cohen R, Cochereau D, Duval A, Lascols O, Lopez-Trabada D, Afchain P, Trouilloud I, Parc Y, Lefevre JH, Flejou JF, Svrcek M, Andre T. Immunotherapy and patients treated for cancer with microsatellite instability. Bull Cancer 2016.
[62] Schwitalle Y, Kloor M, Eiermann S, Linnebacher M, Kienle P, Knaebel HP, Tariverdian M, Benner A, von Knebel Doeberitz M. Immune response against frameshift-induced neopeptides in HNPCC patients and healthy HNPCC mutation carriers. Gastroenterology 2008;134:988-97.
[63] Kim SW, Roh J, Park CS. Immunohistochemistry for Pathologists: Protocols, Pitfalls, and Tips. J Pathol Transl Med 2016;50:411-8.
[64] Stelloo E, Jansen AM, Osse EM, Nout RA, Creutzberg CL, Ruano D, Church DN, Morreau H, Smit VT, van Wezel T, Bosse T. Practical guidance for mismatch repair-deficiency testing in endometrial cancer. Ann Oncol 2016.
[65] Duval A, Reperant M, Compoint A, Seruca R, Ranzani GN, Iacopetta B, Hamelin R. Target gene mutation profile differs between gastrointestinal and endometrial tumors with mismatch repair deficiency. Cancer Res 2002;62:1609-12.

[66] Hause RJ, Pritchard CC, Shendure J, Salipante SJ. Classification and characterization of microsatellite instability across 18 cancer types. Nat Med 2016;22:1342-50.
[67] Boland CR, Thibodeau SN, Hamilton SR, Sidransky D, Eshleman JR, Burt RW, Meltzer SJ, Rodriguez-Bigas MA, Fodde R, Ranzani GN, Srivastava S. A National Cancer Institute Workshop on Microsatellite Instability for cancer detection and familial predisposition: development of international criteria for the determination of microsatellite instability in colorectal cancer. Cancer Res 1998;58:5248-57.
[68] Suraweera N, Duval A, Reperant M, Vaury C, Furlan D, Leroy K, Seruca R, Iacopetta B, Hamelin R. Evaluation of tumor microsatellite instability using five quasimonomorphic mononucleotide repeats and pentaplex PCR. Gastroenterology 2002;123:1804-11.
[69] Loukola A, Eklin K, Laiho P, Salovaara R, Kristo P, Jarvinen H, Mecklin JP, Launonen V, Aaltonen LA. Microsatellite marker analysis in screening for hereditary nonpolyposis colorectal cancer (HNPCC). Cancer Res 2001;61:4545-9.
[70] Ferreira AM, Tuominen I, Sousa S, Gerbens F, van Dijk-Bos K, Osinga J, Kooi KA, Sanjabi B, Esendam C, Oliveira C, Terpstra P, Hardonk M, van der Sluis T, Zazula M, Stachura J, van der Zee AG, Hollema H, Sijmons RH, Aaltonen LA, Seruca R, Hofstra RM, Westers H. New target genes in endometrial tumors show a role for the estrogen-receptor pathway in microsatellite-unstable cancers. Hum Mutat 2014;35:1514-23.
[71] Ferreira AM, Tuominen I, van Dijk-Bos K, Sanjabi B, van der Sluis T, van der Zee AG, Hollema H, Zazula M, Sijmons RH, Aaltonen LA, Westers H, Hofstra RM. High frequency of RPL22 mutations in microsatellite-unstable colorectal and endometrial tumors. Hum Mutat 2014;35:1442-5.
[72] Kim TM, Laird PW, Park PJ. The landscape of microsatellite instability in colorectal and endometrial cancer genomes. Cell 2013;155:858-68.
[73] Novetsky AP, Zighelboim I, Thompson DM, Jr., Powell MA, Mutch DG, Goodfellow PJ. Frequent mutations in the RPL22 gene and its clinical and functional implications. Gynecol Oncol 2013;128:470-4.
[74] Robert J. Kurman MLC, C. Simon Herrington, Robert H. Young. WHO Classification of Tumours of Female Reproductive Organs, 2014.
[75] Greene DLP, Fleming and Fritz AJCC Cancer Staging Manual, 2006.
[76] Ebinger M, Sotlar K, Weber A, Bock CT, Bultmann BD, Kandolf R. Simplified detection of microsatellite instability in colorectal cancer without the need for corresponding germline DNA analysis. J Clin Pathol 2006;59:1114-5.
[77] Carnevali IW, Cimetti L, Sahnane N, Libera L, Cavallero A, Formenti G, Riva C, Tibiletti MG. Two Cases of Carcinosarcomas of the Ovary Involved in Hereditary Cancer Syndromes. Int J Gynecol Pathol 2016.
[78] Joensuu EI, Nieminen TT, Lotsari JE, Pavicic W, Abdel-Rahman WM, Peltomaki P. Methyltransferase expression and tumor suppressor gene methylation in sporadic and familial colorectal cancer. Genes Chromosomes Cancer 2015;54:776-87.
[79] Hong B, Le Gallo M, Bell DW. The mutational landscape of endometrial cancer. Curr Opin Genet Dev 2015;30:25-31.
[80] Banno K, Yanokura M, Iida M, Masuda K, Aoki D. Carcinogenic mechanisms of endometrial cancer: involvement of genetics and epigenetics. J Obstet Gynaecol Res 2014;40:1957-67.
[81] Huang M, Djordjevic B, Yates MS, Urbauer D, Sun C, Burzawa J, Daniels M, Westin SN, Broaddus R, Lu K. Molecular pathogenesis of endometrial cancers in patients with Lynch syndrome. Cancer 2013;119:3027-33.
[82] O'Hara AJ, Bell DW. The genomics and genetics of endometrial cancer. Adv Genomics Genet 2012;2012:33-47.
[83] Beltrame L, Di Marino M, Fruscio R, Calura E, Chapman B, Clivio L, Sina F, Mele C, Iatropoulos P, Grassi T, Fotia V, Romualdi C, Martini P, Noris M, Paracchini L, Craparotta I, Petrillo M, Milani R, Perego P, Ravaggi A, Zambelli A, Ronchetti E, D'Incalci M, Marchini S. Profiling cancer gene mutations in longitudinal epithelial ovarian cancer biopsies by targeted next-generation sequencing: a retrospective study. Ann Oncol 2015;26:1363-71.
[84] Shahsiah R, DeKoning J, Samie S, Latifzadeh SZ, Kashi ZM. Validation of a next generation sequencing panel for detection of hotspot cancer mutations in a clinical laboratory. Pathol Res Pract 2016.
[85] D'Haene N, Le Mercier M, De Neve N, Blanchard O, Delaunoy M, El Housni H, Dessars B, Heimann P, Remmelink M, Demetter P, Tejpar S, Salmon I. Clinical Validation of Targeted Next Generation Sequencing for Colon and Lung Cancers. PLoS One 2015;10:e0138245.
[86] Simen BB, Yin L, Goswami CP, Davis KO, Bajaj R, Gong JZ, Peiper SC, Johnson ES, Wang ZX. Validation of a next-generation-sequencing cancer panel for use in the clinical laboratory. Arch Pathol Lab Med 2015;139:508-17.
[87] Zhang L, Chen L, Sah S, Latham GJ, Patel R, Song Q, Koeppen H, Tam R, Schleifman E, Mashhedi H, Chalasani S, Fu L, Sumiyoshi T, Raja R, Forrest W, Hampton GM, Lackner MR,

Hegde P, Jia S. Profiling cancer gene mutations in clinical formalin-fixed, paraffin-embedded colorectal tumor specimens using targeted next-generation sequencing. Oncologist 2012;19:336-43.
[88] Goodfellow PJ, Billingsley CC, Lankes HA, Ali S, Cohn DE, Broaddus RJ, Ramirez N, Pritchard CC, Hampel H, Chassen AS, Simmons LV, Schmidt AP, Gao F, Brinton LA, Backes F, Landrum LM, Geller MA, DiSilvestro PA, Pearl ML, Lele SB, Powell MA, Zaino RJ, Mutch D. Combined Microsatellite Instability, MLH1 Methylation Analysis, and Immunohistochemistry for Lynch Syndrome Screening in Endometrial Cancers From GOG210: An NRG Oncology and Gynecologic Oncology Group Study. J Clin Oncol 2015;33:4301-8.
[89] Soslow RA. Practical issues related to uterine pathology: staging, frozen section, artifacts, and Lynch syndrome. Mod Pathol 2016;29 Suppl 1:S59-77.
[90] McConechy MK, Talhouk A, Li-Chang HH, Leung S, Huntsman DG, Gilks CB, McAlpine JN. Detection of DNA mismatch repair (MMR) deficiencies by immunohistochemistry can effectively diagnose the microsatellite instability (MSI) phenotype in endometrial carcinomas. Gynecol Oncol 2015;137:306-10.
[91] Rubio I, Ibanez-Feijoo E, Andres L, Aguirre E, Balmana J, Blay P, Llort G, Gonzalez-Santiago S, Maortua H, Tejada MI, Martinez-Bouzas C. Analysis of Lynch Syndrome Mismatch Repair Genes in Women with Endometrial Cancer. Oncology 2016;91:171-6.
[92] Berends MJ, Wu Y, Sijmons RH, Mensink RG, van der Sluis T, Hordijk-Hos JM, de Vries EG, Hollema H, Karrenbeld A, Buys CH, van der Zee AG, Hofstra RM, Kleibeuker JH. Molecular and clinical characteristics of MSH6 variants: an analysis of 25 index carriers of a germline variant. Am J Hum Genet 2002;70:26-37.
[93] Sijmons RH, Greenblatt MS, Genuardi M. Gene variants of unknown clinical significance in Lynch syndrome. An introduction for clinicians. Fam Cancer 2013;12:181-7.
[94] Moller P, Seppala T, Bernstein I, Holinski-Feder E, Sala P, Evans DG, Lindblom A, Macrae F, Blanco I, Sijmons R, Jeffries J, Vasen H, Burn J, Nakken S, Hovig E, Rodland EA, Tharmaratnam K, de Vos Tot Nederveen Cappel WH, Hill J, Wijnen J, Green K, Lalloo F, Sunde L, Mints M, Bertario L, Pineda M, Navarro M, Morak M, Renkonen-Sinisalo L, Frayling IM, Plazzer JP, Pylvanainen K, Sampson JR, Capella G, Mecklin JP, Moslein G. Cancer incidence and survival in Lynch syndrome patients receiving colonoscopic and gynaecological surveillance: first report from the prospective Lynch syndrome database. Gut 2015.
[95] Pineda M, Mur P, Iniesta MD, Borras E, Campos O, Vargas G, Iglesias S, Fernandez A, Gruber SB, Lazaro C, Brunet J, Navarro M, Blanco I, Capella G. MLH1 methylation screening is effective in identifying epimutation carriers. Eur J Hum Genet 2012;20:1256-64.
[96] Lof-Ohlin ZM, Nilsson TK. Pyrosequencing assays to study promoter CpG site methylation of the O6-MGMT, hMLH1, p14ARF, p16INK4a, RASSF1A, and APC1A genes. Oncol Rep 2009;21:721-9.
[97] Mas-Moya J, Dudley B, Brand RE, Thull D, Bahary N, Nikiforova MN, Pai RK. Clinicopathological comparison of colorectal and endometrial carcinomas in patients with Lynch-like syndrome versus patients with Lynch syndrome. Hum Pathol 2015;46:1616-25.
[98] Buchanan DD, Rosty C, Clendenning M, Spurdle AB, Win AK. Clinical problems of colorectal cancer and endometrial cancer cases with unknown cause of tumor mismatch repair deficiency (suspected Lynch syndrome). Appl Clin Genet 2014;7:183-93.
[99] Le Gallo M, O'Hara AJ, Rudd ML, Urick ME, Hansen NF, O'Neil NJ, Price JC, Zhang S, England BM, Godwin AK, Sgroi DC, Hieter P, Mullikin JC, Merino MJ, Bell DW. Exome sequencing of serous endometrial tumors identifies recurrent somatic mutations in chromatin-remodeling and ubiquitin ligase complex genes. Nat Genet 2012;44:1310-5.
[100] McConechy MK, Ding J, Cheang MC, Wiegand KC, Senz J, Tone AA, Yang W, Prentice LM, Tse K, Zeng T, McDonald H, Schmidt AP, Mutch DG, McAlpine JN, Hirst M, Shah SP, Lee CH, Goodfellow PJ, Gilks CB, Huntsman DG. Use of mutation profiles to refine the classification of endometrial carcinomas. J Pathol 2012;228:20-30.
[101] Suhaimi SS, Ab Mutalib NS, Jamal R. Understanding Molecular Landscape of Endometrial Cancer through Next Generation Sequencing: What We Have Learned so Far? Front Pharmacol 2016;7:409.
[102] Loeb LA. Human Cancers Express a Mutator Phenotype: Hypothesis, Origin, and Consequences. Cancer Res 2016;76:2057-9.
[103] Fang M, Hutchinson L, Deng A, Green MR. Common BRAF(V600E)-directed pathway mediates widespread epigenetic silencing in colorectal cancer and melanoma. Proc Natl Acad Sci U S A 2016;113:1250-5.
[104] Fang M, Ou J, Hutchinson L, Green MR. The BRAF oncoprotein functions through the transcriptional repressor MAFG to mediate the CpG Island Methylator phenotype. Mol Cell 2014;55:904-15.
[105] Serra RW, Fang M, Park SM, Hutchinson L, Green MR. A KRAS-directed transcriptional silencing pathway that mediates

the CpG island methylator phenotype. Elife 2014;3:e02313.
[106] Risinger JI, Hayes AK, Berchuck A, Barrett JC. PTEN/MMAC1 mutations in endometrial cancers. Cancer Res 1997;57:4736-8.
[107] Takeda T, Banno K, Okawa R, Yanokura M, Iijima M, Irie-Kunitomi H, Nakamura K, Iida M, Adachi M, Umene K, Nogami Y, Masuda K, Kobayashi Y, Tominaga E, Aoki D. ARID1A gene mutation in ovarian and endometrial cancers (Review). Oncol Rep 2016;35:607-13.
[108] Allo G, Bernardini MQ, Wu RC, Shih Ie M, Kalloger S, Pollett A, Gilks CB, Clarke BA. ARID1A loss correlates with mismatch repair deficiency and intact p53 expression in high-grade endometrial carcinomas. Mod Pathol 2014;27:255-61.
[109] Cheung LW, Hennessy BT, Li J, Yu S, Myers AP, Djordjevic B, Lu Y, Stemke-Hale K, Dyer MD, Zhang F, Ju Z, Cantley LC, Scherer SE, Liang H, Lu KH, Broaddus RR, Mills GB. High frequency of PIK3R1 and PIK3R2 mutations in endometrial cancer elucidates a novel mechanism for regulation of PTEN protein stability. Cancer Discov 2011;1:170-85.

ACKNOWLEDGEMENT:

Unit of Anatomical Pathology:

Prof. Fausto Sessa

Prof. Cristina Riva

Dr. Laura Cimetti

Dr. Anna Maria Chiaravalli

Dr. Simona De Rosa

Molecular Biology Lab:

Dr. Daniela Furlan

Dr. Nora Sahnane

Dr. Roberta Cerutti

Dr. Chiara Albeni

Dr. Daniele Sabatino

Giuseppe Borgia

Oncological Genetic Counselling Service

Dr. Maria Grazia Tibiletti

Dr. Ileana Carnevali

National Cancer Institute, CRO :

Dr. Alessanera Viel (CRO Aviano)

"Mario Negri" Institute for Pharmacological Research:

Dr. Sergio Marchini

Dr. Ilaria Craparotta

Dr. Luca Beltrame

Dr. Laura Mannarino

Ward of Gynecology A:

Prof. Fabio Ghezzi

Dr. Thomas Rossi

Dr. Giorgio Formenti

ACADEMIC RESULTS ACHIEVED DURING THE PhD TRAINING

PUBBLICATIONS

- Carnevali IW, Cimetti L, Sahnane N, **Libera L**, Cavallero A, Formenti G, Riva C, Tibiletti MG. "Two Cases of Carcinosarcomas of the Ovary Involved in Hereditary Cancer Syndromes" Int J Gynecol Pathol (2016)
- Furlan D, Trapani D, Berrino E, Debernardi C, Panero M, **Libera L**, Sahnane N, Riva C, Tibiletti MG, Sessa F, Sapino A and Venesio T. "Oxidative DNA damage induces hypomethylation in a compromised base excision repair colorectal tumorigenesis" accepted by British Journal of Cancer
- Sahnane N, Imperatori AS, Rotolo N, Franzi F, Nardecchia E, **Libera L**, Romualdi C, Cattoni M, Sessa F, Dominioni L, Furlan "LINE-1 hypomethylation is associated to specific clinico-pathological features in Stage I non-small cell lung cancer" submitted to Lung Cancer
- **Libera L**, Sahnane N, Carnavali IW, Cimetti L, Cerutti R, Chiaravalli AM, Riva C, Tibiletti MG, Sessa F, Furlan D. "Technical aspects to improve MSI evaluation of gynecological cancer in daily practice" submitted to Journal of Clinical Pathology
- Carnevali IW, **Libera L**, Chiaravalli AM, Sahnane N, Furlan D, Viel A, Cini G, Cimetti L, Rossi T, Formenti G, Ghezzi F, Riva C, Sessa F, Tibiletti MG "Somatic tests on gynaecological cancers improve the identification of Lynch Syndrome" submitted to European Journal Of Cancer

ABSTRACTS

- Carnevali I, Sahnane N, Chiaravalli AM, Furlan D, Viel A, Cimetti L, **Libera L**, Sessa F, Riva C, Tibiletti MG. "Gynecologic cancer (GC), a "sentinel cancer" for Lynch syndrome (LS)" European Human Genetics Conference 2014 ESHG and VII SIGU Conference, Milan 28 May-1June 2014. Eur J Hum Genet 22 (suppl.1) P18.28-M
- Berrino E, Sahnane N, **Libera L**, Sessa F, Risio M, Furlan D and Venesio T "DNA global demethylation in *MUTYH*-associated polyposis lesions" XII AIFEG Conference, Varese 16-17 October 2014.

- **Libera L** , Carnevali I, Cimetti L, Sahnane N, Chiaravalli AM, Furlan D, Rossi T, Viel A, Sessa F, Riva C, Tibiletti MG. "Uterine cancer in Lynch syndrome: clinico-pathological and molecular features" European Human Genetics Conference 2015 ESHG, Glasgow 6-9 June 2015. Eur J Hum Genet 23 (suppl. 1) PM 12.096

- Berrino E, Panero M, Trapani D, **Libera L**, Sahnane N, Tibiletti MG, Debernardi C, Furlan D, Venesio T. "MAPK pathway mutations and DNA hypomethylation are both involved in the onset of MUTYH associated colorectal carcinogenesis" XIII AIFEG Conference, Naples October 2015.

- **Libera L**, Carnevali IW, Cimetti L, Sahnane N, Rossi T, Formenti G, Chiaravalli A, Furlan D, Riva C, Tibiletti MG. "Ovarian carcinomas and hereditary cancer syndromes" European Human Genetics Conference 2016 ESHG, Barcelona 21-24 May 2016. Eur J Hum Genet 24 (E-Suppl. 1) P12.171

- De Rosa S, **Libera L**, Magnoli F, Capella C, Sessa F, Chiaravalli AM. "PD-L1/PD-1 pathway activation in EBV+ and MSI gastric cancers" XXXI International Congress of the International Academy of Pathology and 28th Congress of the European Society of Pathology, Cologne 25-29 September 2016. Virchows Archiv, Eur J Path 469 (suppl. 1) PS-16-101

CONFERENCE, COURSE AND SEMINARY

- EPIGEN-MiChroNetwork Chromatin Seminar "Drug targeting of the epigenome" Pavia 21 Jenuary 2014
- Seminary "Genomica, Next Generation Sequencing, Bioinformatica: le piattaforme" Varese 25 February 2014
- Seminary "Parterogenesi: vita ed evoluzione senza sesso" Varese 12 March 2014
- Workshop MLPA "Analisi, elaborazione dei dati e troubleshooting della tecnica MLPA", Milano 30 May 2014
- Course "Introduction to Systems Biology", Busto Arsizio 15-22-29 September 2014
- 12° AIFEG Conference, Gazzada Schianno (VA) 16-17 October 2014
- Course of "BIOSTATISTICA" UNINSUBRIA, Varese 9-10-16-17-23-24 March 2015
- Course of "Targeting Lung Cancer" Ospedale di Circolo Fondazione Macchi, Varese 30 March 2015
- Seminary "Watching at the D side: D-amino acids in physiology and pathology" UNINSUBRIA, Varese 15 April 2015

- English course using the platform “Tell me more” UNINSUBRIA, Varese
- 49° ESHG Conference, Glasgow 6-9 June 2015
- Workshop Abbott Molecular “Tumori solidi e FISH: attualità ed esperienze a confronto”, Milan 6 October 2015
- Seminary “PhD thesis: General and regulatory aspects”, Varese 29 February 2016
- 50° ESHG Conference, Barcelona 21-24 May 2016
- Course “Sindrome di suscettibilità ereditaria ai tumori mammari e ovarici: UPDATE 2016”, Varese 17 June 2016
- EMBO Conference "Translational research in cancer cell metabolism", Bilbao 4-6 October 2016
- Online course “WEBINAR: MEET..IMMUNO PATHOLOGY IN CLINICAL PRACTICE 2016, i processi immunologici alla base dello sviluppo dei tumori”, 12 October 2016